PLOS ONE

RESEARCH ARTICLE

In silico analyses and global transcriptional profiling reveal novel putative targets for Pea3 transcription factor related to its function in neurons

Başak Kandemir[1,2], Ugur Dag[2¤a], Burcu Bakir Gungor[3¤c], İlknur Melis Durasi[1,3], Burcu Erdogan[2¤b], Eray Sahin[1,2], Ugur Sezerman[3¤d], Isil Aksan Kurnaz[1,4]*

1 Gebze Technical University, Department of Molecular Biology and Genetics, Kocaeli, Turkey, **2** Yeditepe University, Biotechnology Graduate Program, Kayisdagi, Istanbul, Turkey, **3** Sabanci University, Faculty of Engineering and Natural Sciences, Istanbul, Turkey, **4** Gebze Technical University, Institute of Biotechnology, Kocaeli, Turkey

¤a Current address: Howard Hughes Medical Institute, Janelia Research Campus, Ashburn, Virginia, United States of America
¤b Current address: Boston College, Department of Biology, Chestnut Hill, Massachusetts, United States of America
¤c Current address: Abdullah Gül University, Department of Computer Engineering, Faculty of Engineering, Kayseri, Turkey
¤d Current address: Acibadem University, Faculty of Medicine, Istanbul, Turkey
* ikurnaz@gtu.edu.tr

Citation: Kandemir B, Dag U, Bakir Gungor B, Durasi İM, Erdogan B, Sahin E, et al. (2017) *In silico* analyses and global transcriptional profiling reveal novel putative targets for Pea3 transcription factor related to its function in neurons. PLoS ONE 12(2): e0170585. doi:10.1371/journal.pone.0170585

Editor: Jinsong Zhang, Saint Louis University School of Medicine, UNITED STATES

Received: May 20, 2016

Accepted: January 8, 2017

Published: February 3, 2017

Data Availability Statement: All relevant data are within the paper and microarray data are submitted to EBI ArrayExpress (Experiment ArrayExpress accession: E-MTAB-5324; Title: Expression analysis of Pea3 overexpression in SH-SY5Y cell line; Specified release date: 2016-12-15).

Funding: Support was provided by TUBITAK BIDEB project grants to UD and BE; TUBITAK grants no 107S064 and 214Z278 to IK. The funders had no role in study design, data collection

Abstract

Pea3 transcription factor belongs to the PEA3 subfamily within the ETS domain transcription factor superfamily, and has been largely studied in relation to its role in breast cancer metastasis. Nonetheless, Pea3 plays a role not only in breast tumor, but also in other tissues with branching morphogenesis, including kidneys, blood vasculature, bronchi and the developing nervous system. Identification of Pea3 target promoters in these systems are important for a thorough understanding of how Pea3 functions. Present study particularly focuses on the identification of novel neuronal targets of Pea3 in a combinatorial approach, through curation, computational analysis and microarray studies in a neuronal model system, SH-SY5Y neuroblastoma cells. We not only show that quite a number of genes in cancer, immune system and cell cycle pathways, among many others, are either up- or down-regulated by Pea3, but also identify novel targets including ephrins and ephrin receptors, semaphorins, cell adhesion molecules, as well as metalloproteases such as kallikreins, to be among potential target promoters in neuronal systems. Our overall results indicate that rather than early stages of neurite extension and axonal guidance, Pea3 is more involved in target identification and synaptic maturation.

and analysis, decision to publish, or preparation of the manuscript.

Competing Interests: The authors have declared that no competing interests exist.

Introduction

ETS domain transcription factors are characterized by an evolutionarily-conserved ETS domain of about 85 amino acids that facilitates binding to DNA sequences with a central GGAA/T core consensus and flanking nucleotides [1]. Around 30 members of the ETS proteins have been identified in mammals and are categorized within several subfamilies. Among them, PEA3 subfamily members, most notably Pea3/ETV4, Erm/ETV5 and Er81/ETV1, also bind to the DNA core sequence GGAA/T [2], and contain an acidic activation domain in the N-terminus as well as a C-terminal activation domain [3]. Pea3 family members are involved in several processes, including breast cancer, prostate cancer [4], motor neuron connectivity and dendritic arborization [5] as well as neuronal differentiation [6,7].

Pea3/ETV4 is highly expressed in Her/Neu expressing breast cancer cells and tissues, and the major targets for Pea3/ETV4 previously identified in these tissues were matrix metalloprotease enzymes, particularly MMP1, MMP2 and MMP9, which are required for the initiation of cell migration [8]. In addition, overexpression of Pea3/ETV4 was shown to result in increased levels of vimentin [9], the intercellular adhesion molecule ICAM-1 [10,11], osteopontin [12], vascular endothelial growth factor and cyclooxygenase-2 [13], thus providing evidence for the importance of PEA3/ETV4 in tumor formation and metastasis. But although much is known about how PEA3/ETV4 is involved in breast or prostate cancer [14], very little is understood about how it regulates motor neuron connectivity, retinal development or ganglion cell differentiation [15,16], or indeed which promoters are Pea3 targets in the nervous system. In *C. elegans*, ETS protein Ast-1 (axon steering defect-1) was shown to regulate dopaminergic neuron differentiation through regulating some of the major dopaminergic genes with *ets* motifs [17], but no such targets are yet identified for ETS proteins in mammalian dopaminergic differentiation. On the other hand, cadherin-8, ephrin receptor 4 (Ephr4) and semaphorin-3E were shown to be Pea3 targets in neurons ([16, 18]; also confirmed in this study).

To reveal the possible neuronal targets of Pea3, in this study we have taken the following complementary approach:

Firstly, we have manually curated neural differentiation- and axon guidance-related promoter sequences and analyzed the selected promoter reqions for the selected transcription factor.

Secondly, we have developed an automated tool to identify all promoters that contain the binding site for a given transcription factor. Although this approach is less labor-intensive compared to the prior strategy of manual curation, it is limited to the entries within the existing promoter databases. Yet, our study shows that there is significant overlap between these two *in silico* target identification approaches.

Thirdly, we have conducted microarray analyses, where we have not only confirmed a subset of genes identified in the above-mentioned *in silico* analyses, but also identified many more potential novel targets for Pea3 transcription factor. These novel targets include several genes that function in cytoskeletal organization, axon guidance, cell migration, ion channels, enzymes and signaling pathway components, as well as many others. KEGG pathway-based analysis of microarray data also showed a significant number of novel genes in neurotrophin signaling pathway, MAPK pathway, glioma pathway and long-term potentiation, among many others. A small subset of these were further analyzed and confirmed through qRT-PCR analysis, and *in silico* tools predicted high affinity binding sites for Pea3 in their promoters.

One important finding is the mixed nature of Pea3 transcriptional activity—while it activated some of these novel target promoters, it was found to repress others. We do not as yet know the detailed mechanism of this regulation, ie whether there are coactivators or corepressors involved, or if posttranslational modifications of Pea3 render it as an activator or a

repressor, or indeed whether there is an indirect regulation through activation of miRNA genes that in turn repress some of these promoters [21]. Nonetheless, the analysis of the small subset or target genes presented in this study indicate that rather than regulating axonal outgrowth and guidance, Pea3 is more likely to be involved in target recognition, growth cone collapse, and/or synaptic maturation, and involved in endocytosis as well as synaptic vesicle cycle. This is in line with previous findings that Pea3 family members function at later rather than earlier stages of neuronal differentiation.

Materials and methods

Curation of potential target promoters for analysis

Since this study is concerned primarily with identification of novel target promoters of Pea3/ETV4 with respect to the nervous system development, we were mainly focused on potential target genes involved in "neuronal migration" and "axonal guidance"; these two phrases were used as our gene search parameter. The genes searched for these criteria have been identified by means of "Gene" tool of NCBI (http://www.ncbi.nlm.nih.gov/gene/). The promoter sequences that correspond to these curated set of genes were then retrieved from the Transcriptional Regulatory Element Database, TRED (http://rulai.cshl.edu/cgi-bin/TRED/tred.cgi?process=home; [19]). This website has a genome-wide database for the promoter sequences, and using the transcription start site (TSS) setting, the target promoter sequences were displayed from -700 to +300 base pairs relative to TSS (Fig 1a).

Analysis of the promoter sequences for Transcription Factor Binding

The promoter sequences manually obtained from TRED were analyzed with PROMO 3.0 (http://alggen.lsi.upc.es/cgi-bin/promo_v3/promo/promoinit.cgi?dirDB=TF_8.3; Fig 1a). PROMO 3.0 tool analyzes the promoter regions for binding by a selected transcription factor, and displays the results with a "dissimilarity rate" [20]. Dissimilarity rate simply implies the variance between the binding motif of the transcription factor and the nucleotide sequence on the promoter as percentage by regarding the binding matrices. From this point of view, the smaller dissimilarity rates are the indicators of higher possibility for Pea3/ETV4 binding (0% dissimilarity rate shows 100% identity to consensus motif). To confirm the reliability of this method, promoter sequences for matrix metalloproteases MMP3 and MMP9 as well as Vascular Endtothelial Growth Factor (VEGF), the known targets for Pea3/ETV4 [13, 22, 23] were used as positive controls, with dissimilarity rates determined to be 0% as expected (data not shown).

Development of a promoter analysis tool

While the above manual analysis requires the user to find and define selected subset of promoter sequences from any nucleotide database and analyze it for presence or absence of one particular Transcription Factor (TF) binding motif (promoter by promoter), an automated tool was designed to obtain the promoter sequences of all human genes (user-defined range, eg 1000 bp upstream) using biomaRt R package [24,25] http://www.ensembl.org/info/data/biomart/biomart_r_package.html).

In the first step, the automation tool retrieves all human protein coding genes with their Entrez IDs and gene names from the Ensembl database (http://www.ensembl.org). In the second step, using the human gene list, promoter regions are selected among these sequences according to the user defined criteria. In the third step, using MotifDB R library [26] (http://bioconductor.org/packages/release/bioc/html/MotifDb.html), position weight matrices

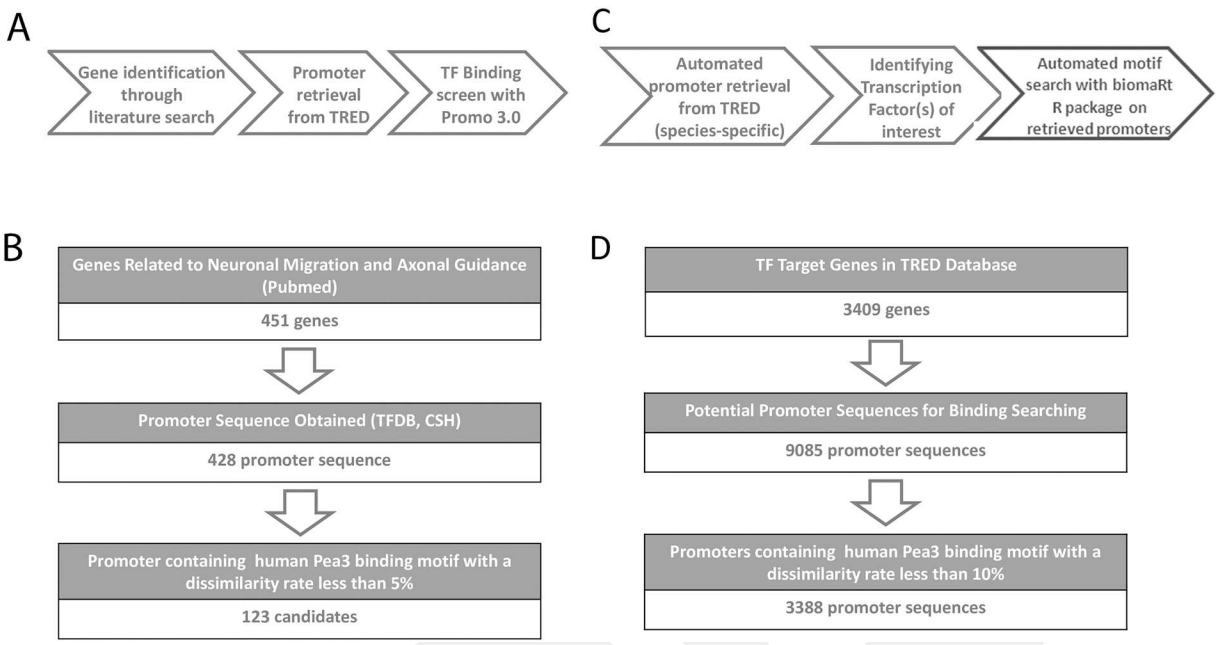

Fig 1. (a) and (b) Experimental flowchart and summary of manual curation-based promoter analysis; (c) and (d) Experimental flowchart and summary of automated promoter analysis. (a) Genes of interest were manually curated and determined using PubMed and NCBI Gene tools; corresponding promoters were retrieved from TRED database, followed by screening for transcription factor (TF, in this case Pea3) binding using Promo 3.0 tool (see text for details); (b) With respect to neuronal migration and axonal guidance, a total of 451 genes were identified, for which only 428 promoters were retrieved. Upon analysis, only 123 possible candidate promoters were identified to contain Pea3 binding motif with a dissimilarity rate of less than 5%; (c) upon development of the automation program, it was used to retrieve promoters from TRED in a species-specific manner, followed by identification of the transcription factor(s) of interest by the user, whose binding motifs were searched using Promo 3.0 tool (see text for details); (d) a total of 3409 genes and a corresponding 9085 promoters (multiple promoter entries were possible for some genes) were retrieved and analyzed, which yielded 3388 promoter sequences that contain Pea3 binding motif with a dissimilarity rate of less than 10%.

doi:10.1371/journal.pone.0170585.g001

(PWM) for any transcription factor are retrieved [27]. (For our specific application in this study, etv4 PWM is retrieved to define Pea3 binding motifs on promoters.) The algorithm then searches in the promoter regions for the presence of subsequences with a minimum matching score of 80% to the PWM selected. All promoters with predicted etv4 binding motifs are reported in this study.

Cell culture and transfection

SH-SY5Y human neuroblastoma cell line (ATCC(®) CRL-2266™) is typically maintained in the high glucose DMEM (Gibco, 1129855) supplemented with 10% Fetal Bovine serum (Life Technologies, 10500–064) in the presence of penicillin, streptomycin, L-Glutamine and amphotericin B (Biological Industries, 03-033-1B) and primocin (Invivogen, ant-pm-1). For transfection, SH-SY5Y cells were seeded at 1.5 million cells per 10 cm diameter dish, and 24 hr later transfected with either pCDNA3 and pCDNA3-mPea3-VP16 (courtesy of Prof. A.D. Sharrocks) using the PEI reagent (CellnTech), in 3 replicas per sample.

RNA isolation, cDNA synthesis, Reverse Transcription Polymerase Chain Reaction (RT-PCR) and Real-Time PCR

Total cytoplasmic RNA is commonly prepared using RNAeasy kit (Qiagen, cat no 74104) as per manufacturer's instructions. 1 μg RNA was used for each first strand cDNA synthesis reaction (M-Mu-LV-Rtase, Roche) as per manufacturer's instructions, using random primers

(Boehringer Mannheim). The amount of cDNA used was standardized using GAPDH and linear range was determined. Typically the RT-PCR reactions were performed using 10–50 ng cDNA template in 20 μl reaction with BioTaq polymerase at 54.5˚C for 30 cycles. For conventional PCR, the products were resolved in 2.5% Nu-Sieve) agarose gels and were analyzed using QuantityOne imaging software (BioRad).

On the other hand, 40 ng cDNA template in 10 μl reaction with IQ SYBR green super mix (BioRad, cat no 170–8880) was used for Real-time polymerase chain reaction (qRT-PCR) and carried out using a CFX96 Touch Real-Time PCR detection system. To evaluate whether the difference in gene expression level between control and transfected cells was significant, the efficiency (E) -corrected delta cycle threshold (ΔCt) method was used according to the formula:

$$\text{relative quantity } (\text{RQ})_{\text{target}} = \frac{Etarget^{Ct(pCDNA3)-Ct(Pea3-VP16)}}{Egapdh^{Ct(pCDNA3)-Ct(Pea3-VP16)}}$$

The RQ values thus calculated were then transformed on a log2 scale to achieve normal distribution of the data and the resulting distributions were tested against the null-hypothesis of equal mRNA level in control and transfected cells (i.e., a population mean of 0.0) using two-tailed one-sample Student's t-tests. An α-level of ≤ 0.05 was applied for all comparisons to determine statistical significance.

The list of primers used in RT-PCR and qRT-PCR are shown in Table 1.

Microarray and data analysis

For microarray analysis, SH-SY5Y cells were transfected as described above, and 48 hr after transfection RNA samples were isolated using Ambion Tri-pure RNA isolation kit, checked for quality, converted to cDNA and confirmed for Pea3 expression as described above. Thereafter, RNA was converted to cDNA using the *Superscript Double-stranded cDNA Synthesis (Invitrogen)* Kit and labeled with *NimbleGen One Color DNA Labeling* (NimbleGen, Roche). The labeled cDNA were hybridized to NimbleGen Human Gene Expression Array 12x135K (NimbleGen, Roche), which covers 45.033 genes with 3 probes per gene, containing 12 arrays per slide. After hybridization, slides were scanned using Genepix 4000B scanner and analyzed with NimbleScan 2.5 software using three arrays from pCDNA3-transfected cell as reference samples. The averaged fold changes and p values for each gene were calculated, and genes which were up- or down-regulated, with FDR (False Discovery Rate) adjusted p value of 0.05 or less were assumed to be significant [28]. Data was submitted to EBI ArrayExpress, accession E-MTAB-5324.

Gene IDs were converted to official gene symbol, then *Kyoto Encyclopedia of Genes and Genomes* (KEGG) pathway tools were used for functional enrichment of the list of genes and identification of affected pathways and processes. KEGG pathway tools were analyzed through both PANOGA online tool (http://panoga.sabanciuniv.edu/index.html; Sezerman Lab) using STRING protein protein interaction database (http://string-db.org/newstring_cgi/show_input_page.pl; free). Genes with p-values (significance values) smaller than 0.05 were listed and used for further analysis. PANOGA maps the list of genes and their significance values to STRING PPI network and identifies active subnetworks involving most of the affected genes by PEA. Then it identifies affected KEGG pathways within these subnetworks and assigns significance to them based on hypergeometric distribution.

Table 1. The list of primers used in qRT-PCR analyses (* primer sequences obtained from Pratt and Kinch, 2003).

Gene	Forward Primer (5'>3')	Reverse Primer (5'>3')
KLK2	GATTGTGGGAGGCTGGGAGTGTGAG	GGACAGGAGATGGAGGCTCACACAC
KLK3	AGC GTG ATC TTG CTG GGT CG	CCTTGAAGCACACCATTACAGAC
KLK4	ATT GTT CTG CTC GGG CGT CCT G	GGGTCTGTTGTACTCTGGGTGC
KLK5	GCA TCC ACA GTG GCT GCT CA	TGAGCATGAGGTTGTTAGAGTGGC
KLK6	GGG TCC TTA TCC ATC CAC TGT G	TGGCGGCATCATAGTCAGGGTG
KLK7	GGA ACC ACC TGT ACT GTC TCC	TTTCTTGGAGTCGGGGATGCC
KLK8	TTG TAG GTG GCA ACT GGG TCC	CTGGTCACGCAGTTGAAGAAGC
KLK9	CTC AAC CTC AGC CAG ACC TGT GT	TGCTGTCCGAGATGTGTCCAG
GRIK3	TGAACCTCTACCCCGACTACG	ATGGGGAGCTGACGGATCTTCAG
GLUD2	GAATGCTGGAGGAGTGACAGTATC	GCAGAACGCTCCATTGTGTATG
EFNB2	GCAAGTTCTGCTGGATCAAC	AGGATGTTGTTCCCCGAATG
EFNB1	GGAGGCAGACAAACATGTCA	GAACAATGCCACCTTG
EFNA3	CCACTCTCCCCCAGTTCACCATG	GCTAGGAGGCCAAGAACGTC
EPHA1	CTGCTGCTTGGTGCAGCCTTG	GCTTCAGCCACAGCTTGTCCTCTCG
EPHA2*	ATGGAGCTCCAGGCAGCCCGC	GCCATACGGGTGTGTGAGCCAGC
L1CAM	GCTGGTTCATCGGCTTTGTG	GTCTCATCTTTCATCGGTCGG
PTK2B	GATGACCTGGTGTACCTCAATG	GTGTGAAGCCGTCAGCATCTG
UNC5A	GCCTTCAAGATCCCCTTCCTC	CTGGGCTTGGAGGCAAAGAAG
SEMA4C	CTGAGAGGACCTTGGTGTACC	GGTGAAGCCGAGTTGGAGAAG
NGFR	GAGAAAAACTCCACAGCGACAGTG	GGTAAAGGAGTCTATGTGCTCGG
FGFR1	GTACATGATGATGCGGGACTGCTG	GAGAAGACGGAATCCTCCCCTGAG

doi:10.1371/journal.pone.0170585.t001

Weblogo analysis

Putative Pea3 binding motifs on a specific subset of promoters were further analyzed using Weblogo version 2.8.2 (http://weblogo.berkeley.edu/logo.cgi). This freely available online tool generates a graphical representation of amino acids or nucleic acids after multiple sequence alignment, where the overall height of the particular residue indicates the degree of conservation of that residue in all sequences analyzed.

Chromatin immunoprecipitation (ChIP) assay

SH-SY5Y cells were plated in 150 mm diameter dishes and twenty four hours later transfected with either empty pCDNA3 or Pea3-VP16 expression plasmid, as described above. Forty eight hours after transfection cells were cross-linked with 1% formaldehyde and lysed in lysis buffer (85 mM KCl, 0,5% NP-40, 20 mM Tris-HCl pH8.0, protease inhibitor cocktail). The lysates were sonicated using Bioruptor Pico (Diagenode) in nuclei isolation buffer (100 mM HEPES, 1,5 mM $MgCl_2$, 10 mM KCl, 1 mM DTT, protease inhibitor coctail). 10% v/v of the sheared DNA was separated as input, and rest of the sample was precipitated using 30 μl of anti-Flag M2 affinity resin (Sigma) or normal mouse IgG (Santa Cruz, sc-2025) overnight. Immunoprecipitated chromatin was washed and eluted in elution buffer (20%SDS, 1M $NaHCO_3$). Cross-linking of proteins and DNA was reversed and treated with RNaseA and proteinase K. DNA was then purified using MEGAquick-spin™ Total Fragment DNA Purification Kit (Intron). Enrichment at promoter sites was detected by qPCR using iTaq Universal SYBR Green Supermix (BioRad). MMP9 promoter region was used as a positive control, and FGFR1 intron region harboring no *ets* motifs served as negative control (data not shown). Primers used in

Table 2. The list of primers used in ChIP qPCR analyses.

Gene ID	Forward (5'-3')	Reverse (5'-3')
Akt1—1	CAGGAAGGCCCATCTGGAAG	CCCTCACCTGAGCACACTTT
Akt1—2	CCCAGGAGGTTTTTGGGCTT	CGTTTGCTCTCCCTGTCCAT
EPHA1—1	CCAACCAGATCAGCCCATGT	CGAGTGGAAGTGCAGGATGT
EPHA1—2	GAGTGGCTCGAGTCCATACG	CTGTGGGCAAGGAAGGGTG
EPHA1—3	AAGGTCGCTCATGGTCACTC	TAACCCCTCAGCTCCCTCC
EPHA2—1	GGGTACCTCAAGCCCCATTT	CAAGCATCTTGCAAAGGCCC
EPHA2—2	AACATTCGTGAGCTGGGGAC	AGACTGAAAGCCAAGATCGGT
FGFR1	TCTCGCAACAGGAAGGAACC	GGGGTTGTGAGTGGAGACAG
L1CAM	GGAGCTCCATACACACGCTG	TCAGACGATAGGGAGGGCAG
MMP2	CCCCTGTTCAAGATGGAGTC	CCCAGGTTGCTTCCTTACCT
Negative	GGACGTGGAGGGCTAGGTTA	TTAACGACCGTGGGTTGTCC
SEMA4C—1	GCCCAAGTGCACCTACGTC	TCCAAAGTGAAGGTGAGCATGT
SEMA4C—2	GTCCCTATGACCCAGCTAAGG	ACCATCTATGGGAGACAGAGGT

doi:10.1371/journal.pone.0170585.t002

ChIP qPCR are listed in Table 2. ChIP-qPCR data was analyzed according to the formula

$$\text{Relative ChIP binding} = 2^{-(Ct[IP]-Ct[Input\times DF])} \times 100\%$$

where Ct is the cycle threshold, IP is the qPCR intensity units obtained from qPCR of chromatin IP samples, Input is that obtained from input, and DF is the dilution factor.

Results and discussion

The aim of this combinatorial study was to identify novel transcriptional targets for Pea3 with respect to its neuron-specific functions. To that end, our first approach was an *in silico* analysis through manual curation of predicted target promoters for Pea3/ETV4 (Fig 1a). 404 human genes related to neuronal migration and 47 human genes related to axonal guidance were manually curated, and promoter sequences for 428 of these were found through nucleotide databases (Fig 1). Out of these, 123 candidate promoters crossed the threshold (5% dissimilarity rate) for Pea3/ETV4 binding (Fig 1b).

When the promoters that contain lower than 5% dissimilarity score for either mouse or human Pea3 binding motifs for both neuronal migration and axonal guidance were compared, it was seen that 19 promoters were common in both functions (Table 3). Among these, 6 of them were seen to be related to adhesion, 10 related to cell-to-cell signaling, 2 were considered to be structural, and 1 was a transcription factor (Table 3). The dissimilarity scores of the promoters of these genes (either from human or mouse promoter database) for Pea3 binding are listed in Table 3, and may differ in a species-specific manner; for example, for SLIT2, Slit homolog 2, mouse Pea3 binding dissimilarity rate was found to be 3,94%, whereas that for human Pea3 was as low as 0,43% (Table 3). SLIT2 is an axonal guidance molecule that appears to be essential for midline crossing in the midbrain as well as spinal cord by modulating the cell's responses to Netrin (http://www.genecards.org/cgi-bin/carddisp.pl?gene=SLIT2), but also important in kidney, inflammation, angiogenesis and glioma migration [29–32], all of which are processes where Pea3/ETV4 is implicated. On the other hand for KAL1, Kallman syndrome 1, the scores were just the opposite, 0,63% for mouse Pea3 and 9,45% for human Pea3 binding (Table 3). KAL1 gene codes for the axonal guidance protein called anosmin 1 particularly involved in the developing brain, and is known to be involved in neurite branching [33] (http://www.genecards.org/cgi-bin/carddisp.pl?gene=ANOS1&keywords=KAL1).

Table 3. The putative Pea3 target genes identified through manual curation with respect to neuronal migration and axon guidance.

Gene symbol	Gene name	Accession #	mPea3	hPea3	Function of genes	REFS
BDNF	Brain Derived Neurotrophic factor	8188	0,63	N/A	Growth factor activity (cell-cell signaling)	[42,85]
CDK5R1	Cyclin Dependent Kinase 5 regulatory subunit 1	115721	N/A	9,45	Calcium ion binding, protein kinase activity (cell-cell signaling)	[87]
CNTN2	Contactin 2	1782	3,94	9,24	Carbonhydrate and glycoprotein binding (adhesion)	[88]
EphA8	Ephrin Receptor A8	318	3,94	N/A	ATP binding, nucleotide binding and receptor activity (cell-cell signaling)	[43,89]
EphB2	Ephrin Receptor B2	323	N/A	9,67	Ephrin receptor activity, nucleotide binding, protein tyrosine kinase activity (cell-cell signaling)	[90]
GNAI2	Guanine nucleotide binding protein (G protein) alpha inhibiting activity polypeptide 2	29399	1,70	9,67	GTPase activity, signal transducer (cell-cell signaling)	[91]
KAL1	Kallmann syndrome 1 sequence	44617	0,63	9,45	Extracellular matrix structural constituent (structural)	[34, 92]
L1CAM	L1 Cell adhesion molecule	113184	0,63	0	Identical protein binding (adhesion)	[34,93]
MAPK8IP3	mitogen-activated protein kinase 8 interacting protein 3	14609	3,94	7,14	MAP kinase scaffold activity (cell-cell signaling)	[94]
MYH10	myosin, heavy chain 10, non-muscle	19064	6,61	N/A	Actin binding, microfilament motor activity (structural)	[95]
NCAM1	Neural Cell Adhesion Molecule 1	7078	0	0,43	Identical protein binding (adhesion)	[96]
NEUROG2	Neurogenin 2	32273	0,63	0,21	Sequence-specific DNA binding (Transcription Factor)	[97]
NGFR	Nerve growth factor receptor	17440	1,70	9,24	Receptor and signal transducer activity (cell-cell signaling)	[98]
NRCAM	Neuronal cell adhesion molecule	38906	8,32	9,67	Ankyrin binding (adhesion)	[99]
Nrp1	Neuropilin 1	5859	3,31	9,24	Growth factor binding (cell-cell signaling)	[100]
NTF3	Neurotrophin 3	8613	0	7,14	Receptor binding (cell-cell signaling)	[101]
PTK2	Protein Tyrosine Kinase 2	116986	0,63	0	Nucleotide binding and signal transducer activity (cell-cell signaling)	[102]
SEMA4A	Semaphorin 4A	1354	3,94	9,67	Receptor activity (adhesion)	[86, 103]
SLIT2	Slit Homolog 2	116382	3,94	0,43	GTPase inhibition, Roundabout binding, calcium ion binding (adhesion)	[29,51,104]

doi:10.1371/journal.pone.0170585.t003

The promoters that consistently had lowest dissimilarity rates for both mouse and human Pea3/ETV4 binding were considered as more likely targets for a consistent and conserved Pea3-dependent regulation: Protein tyrosine kinase 2 (PTK2) exhibited dissimilarity scores of 0,63 for mouse and 0 for human Pea3/ETV4 binding; L1 cell adhesion molecule (L1CAM) exhibited 0,63 dissimilarity score for mouse Pea3 and 0 for human ETV4 binding; Neural cell adhesion molecule 1 (NCAM1) showed 0 dissimilarity for mouse and 0,43 for human Pea3/ ETV4; and Neurogenin 2 (NEUROG2), 0,63 for mouse and 0,21 for human Pea3/ ETV4 binding. Among these, L1CAM was particularly interesting since it was shown to be present in a complex with KAL1-FGFR in regulating neurite branching [33], and also known to regulate axon-axon interaction [34]–KAL1 being the other putative target identified through this method (discussed in the previous paragraph).

Some promoters were only analyzed for mouse or human Pea3 binding, including ephrin receptor B2, ephrin receptor A8, CDK5 regulatory subunit 1, BDNF, and myosin heavy chain 10, since promoter sequence from only one organism's genome could be accessed (Table 3). Ephrins and their receptors are also interesting targets for Pea3 regulation, since they are not

only involved in cell guidance and migration during axonal development, but also in glioblastoma progression [35, 36].

Automated promoter analysis tool

The above analysis was based on a manually curated set of promoters that were identified with respect to their involvement in neuritogenesis, migration and axonal guidance. We next wanted to address whether the automated analysis tool that we developed that screens for an entire promoter database for putative Pea3 binding in an unbiased fashion would result in a similar set of potential target promoters. When this promoter analysis tool was employed (see Materials and Methods for details; Fig 1c), a total of 9085 promoter sequence entries for 3409 genes were retrieved and analyzed for putative Pea3/ETV4 binding (Fig 1d). For this particular genome-wide *in silico* analysis, a higher dissimilarity score of 10% was set as threshold, which resulted in the identification of 3388 promoter sequences positive for Pea/ETV4 binding motifs (Fig 1d).

When the results from this automated tool was compared with manually identified targets for Pea3/ETV4, 57 genes were found to be overlapping, 15 of which had lower than 5% dissimilarity for Pea3/ETV4 binding in both mouse and human promoters (Table 4). Out of these, ANGPT-1 (angiopoietin) is widely known as an endothelial growth factor, and yet it was shown to protect neurons from apoptosis [37]. Similarly, CX3CR1 (chemokine C-X3-C motif receptor 1) is implicated in neuronal survival, where knockout of CX3CR1 in microglia was shown to prevent neuronal loss [38]. Integrin-like kinase (ILK) mediates survival and synaptic plasticity of hippocampal neurons [39]. And the tumor suppressor protein TP53 was shown to play a role in the survival of neural progenitor cells [40].

When Table 3 was further analyzed for genes that could play a role in neuronal differentiation, migration, or axonal guidance, however, a different subset were particularly found to be interesting. Among these, DCLK1 (doublecortin-like kinase) is a protein kinase that is known to be upregulated in response to BDNF signal, and to be involved in neuronal migration and neurogenesis (http://www.ncbi.nlm.nih.gov/gene/9201) [41]; LIMK1 (LIM domain kinase 1) regulates actin cytoskeletal dynamics and was shown to be linked to BDNF-induced neuritogenesis [42]; UNC5B, when bound to netrin-4, is involved in thalamocortical axon branching [43]; and NRXN1 codes for neurexin1 protein that functions in cell adhesion in vertebrate nervous system (http://www.genecards.org/cgi-bin/carddisp.pl?gene=NRXN1).

It should be noted, however, that both manual curation followed by manual *in silico* analysis and automated promoter screening for Pea3/ETV4 binding does not in any way imply that these promoters are genuine targets for Pea3/ETV4 in neurons. Therefore, experimental verification is necessary for both *in silico* approaches.

Microarray analysis of target genes

To experimentally verify the predictions, as well as to identify novel targets for Pea3/ETV4 in neurons, we have carried out a microarray analysis in SH-SY5Y human neuroblastoma cell lines overexpressing mPea3-VP16 fusion protein. When the data were analyzed, quite surprisingly 68.7% of all affected genes were found to be repressed between 2- and 5-fold in cells overexpressing Pea3-VP16 as compared to pCDNA3-transfected cells, with about 23.3% of all affected genes being repressed over 5-fold. Since VP16 is a highly potent activation domain, such a high ratio of repressed genes could either be explained through an indirect repression via activation of specific miRNA genes (which could not be identified in the arrays employed in this study), or through steric hindrance of a critical transactivator from binding when Pea3-VP16 was bound.

Table 4. The putative Pea3 target genes identified *in silico* that are overlapping in both automated analysis and manual curation.

Gene symbol	Gene name	Accession #	mPea3	hPea3
ACTN2	Actinin, alpha 2	2058	0	9,45
ADAM10	ADAM metallopeptidase domain 10	14166	0	9,45
ANGPT-1	Angiopoietin	113693	0	0,43
APC	Adenomatous polyposis coli	33308	0,63	9,45
BMP2	Bone morphogenic protein 2	113729	8,32	9,67
CDH1	Cadherin 1, type 1, E-cadherin (epithelial)	15369	3,94	N/A
CDK5R1	Cyclin-dependent kinase 5, regulatory subunit 1	115721	N/A	9,45
CIB1	Calcium and integrin binding 1 (calmyrin)	13845	4,38	0,21
CSF1	Colony stimulating factor 1 (macrophage)	112668	1,07	9,45
CST3	Tachykinin receptor 1	25458	7,25	N/A
CX3CR1	Chemokine (C-X3-C motif) receptor 1	30958	0,63	0
DCLK1	Doublecortin-like kinase	11447	3,94	7,14
DIAPH1	Diaphanous homolog I (Drosophila)	34180	1,7	0,21
DPYSL2	dihydropyrimidinase-like 2	39825	0,63	7,14
DRD5	Dopamine receptor D5	31284	1,07	7,14
DYX1C1	Dyslexia susceptibility 1 candidate 1	124118	8,32	9,45
EGR1	Early growth response 1	33479	3,31	7,14
FES	Feline sarcoma oncogene	13679	3,31	9,45
GMIP	GEM interacting protein	120115	3,94	N/A
GNB1	Guanine nucleotide binding protein	4136	0	9,24
GNB2L1	G protein, beta polypeptide 2-like 1	33870	N/A	6,93
HSPA4	Heat shock protein 70 kDa protein 4	33414	3,94	0,21
HSPB1	Heat shock 27 kDa protein 1	37879	1,7	N/A
IGFBP3	Insulin-like growth factor binding protein 3	39292	3,31	9,45
ILK	Integrin-linked kinase	6243	0,63	0,43
INS	Insulin	8437	3,94	9,67
IRS2	Insulin receptor substrate 2	11182	N/A	9,45
ITGA5	Integrin, alpha 5 (fibronectin receptor, alpha polypeptide)	10119	0,63	N/A
KAL1	Kalmann syndrome 1 sequence	44617	0,63	9,45
LIMK1	Lim kinase 1	37847	3,94	0
MAP3K5	Mitogen-activated protein kinase kinase kinase 5	36258	0,63	0
MAPK8IP3	Mitogen-activated protein kinase 8 interacting protein 3	14609	3,94	7,14
MMP9	matrix metallopeptidase 9	26338	0	6,93
NDN	Necdin homolog (mouse)	1442	0,63	0
NRAS	Neuroblastoma RAS viral (v-ras) oncogene homolog	3139	3,31	0,21
NRXN1	Neurexin 1	116392	3,31	N/A
PDPK1	3-phosphoinositide dependent protein kinase-1	14469	0	9,45
PRKCA	Protein kinase C, alpha	114871	0	9,45
PTEN	Phosphatase and tensin homolog	4722	1,7	7,36
PTGS2	Prostaglandin-endoperoxide synthase 2	112626	3,94	9,45
PTK2	Protein Tyrosine Kinase 2	116986	0,63	0
PTK2B	Protein tyrosine kinase 2 beta	39829	0	0
PTPN1	Protein tyrosine phosphatase, non-receptor type 1	26382	0	0,21
RB1CC1	RB1-inducible coiled-coil 1	40992	3,31	N/A
RGMA	RGM Domain Family Member B	33277	3,31	N/A
RGMB	RGM Domain Family Member A	13823	3,94	0
RRAS	Related RAS viral (r-ras) oncogene homolog	21730	3,94	7,14

(*Continued*)

Table 4. (*Continued*)

Gene symbol	Gene name	Accession #	mPea3	hPea3
SEMA3B	Semaphorin 3B	29403	0	9,24
SEMA4A	Semaphorin 4A	1354	3,94	9,67
SGK1	Serum/glucocorticoid regulated kinase 1	36274	6,61	6,93
TBX21	T-box 21	17380	0,63	9,67
TP53	Tumor protein p53	19095	3,94	9,45
TPM3	Tropomyosin 3	20450	1,7	9,45
TSC2	Tuberous sclerosis 2	14637	0	0,43
UNC5B	UNC5-homolog b	4599	0	N/A
WASL	Wiskott-Aldirich syndrome-like	38866	6,61	6,93
WT1	Wilm's tumor 1	8172	0,63	9,45

doi:10.1371/journal.pone.0170585.t004

To identify the impact of these changes at cellular level and determine the affected pathways, microarray data were further analyzed in 5 runs of PANOGA. These results were then listed from the most statistically significant pathway to the least: Cell cycle, MAPK signaling pathway and Pathways in cancer, Endocytosis and Neurotrophin signaling pathway appeared in the top five (Table 5). Among the pathways directly related to neural circuit assembly are ECM-receptor interaction and axon guidance pathways, which include genes such as EFNA3, EPHA2, SEMA4C, L1CAM that exhibit high statistical significance in PANOGA analysis (Table 5). Others in these pathways, such as EFNB1, EFNB2, and UNC5A also appear as potential Pea3 targets, albeit with lower significance ($p<0.004$; data not shown). These genes are of particular interest to this study, since they are reported to be directly involved in neural fold fusion, neural differentiation, or axonal guidance in previous reports [44–48].

It is important to note that the presence of endocytosis, focal adhesion, SNARE interactions in vesicular transport, synaptic vesicle cycle, and regulation of actin cytoskeleton pathways among the results (Table 5) indicates that Pea3 may also be reinforcing its role in neural circuit assembly through these pathways. Ephrins, for example, were shown to trigger endocytosis in order to mediate repulsion; similarly, Sema3A-mediated growth cone collapse was shown to occur alongside endocytosis (rev. in [49]). Reorganization of the actin cytoskeleton is a sure must in growth cone guidance and/or collapse (rev. in [49]).

Wnt signaling, Notch signaling, and Hippo signaling pathway components, among many others, were also found to be affected in response to exogenous Pea3-VP16 expression (Table 5). Although Wnt signaling was long known for its role in early embryonic development, their role in growth cone and axon guidance have been identified only a decade ago [50, 51]. Notch signaling is involved in the early development of many systems, nervous system being one—it was shown to be important for axonal outgrowth as well as dendritic patterning in various model systems [52–54]. Hippo pathway, which is known to be a common regulator of organ size in development, was recently shown to mediate ephrinB/EphB signaling in peripheral nerve regeneration [55]. Hippo and Wnt pathways have also been shown to cross-talk in various systems [56], and regulate *Drosophila* photoreceptor fate [57].

There were also quite a number of immune system-related pathways affected by Pea3-VP16 overexpression, such as those in Tumor Necrosis Factor (TNF) signaling pathway, Fc gamma R-mediated phagocytosis, and T cell receptor signaling pathway (Table 5). Immune system has been on the stage for quite some time in several processes from neurogenesis to brain tumors and neurodegeneration [58, 59]. TNF, for example, was shown to inhibit neurite outgrowth in the hippocampus [60]. In addition, presence of active T cells were found to be crucial for

Table 5. PANOGA analysis of microarray results. Data was run 5 times, and genes with statistical significance were reported for occurrence and name. Pathways of interest are indicated in **bold**.

Pathways	p-value	Occurrence	Affected Genes
Cell cycle	4,18748E-21	5	RB1, PKMYT1, FZR1, CCND1, YWHAQ, E2F1, CDC25A
MAPK signaling pathway	**7,39475E-19**	**5**	**MAX, ARRB1, ARRB2, DUSP16, ELK1, RELA, RELB, RPS6KA4, RPS6KA3, MAPK1, RAC3, CACNG2, DUSP4, MAP3K3, JUND, TRAF2, DUSP7, TAOK2, MAP3K11, FGFR1**
Pathways in cancer	1,11864E-17	4	RB1, RET, PIK3R2, RELA, RXRB, CCND1, GNA11, DVL2, E2F1, MAPK1, RAC3, FADD, PLCG1, VHL, RALGDS, APC2, JUP, DAPK3, ARNT, AXIN2, RARA, ARHGEF1, FGFR1
Endocytosis	**4,6808E-14**	**5**	**RET, AP2A1, AP2A2, GIT1, SH3GL1, AP2B1, VPS37B, SMAD6, DNM1, EPN1, DNM2, EPN2, RAB11B, SMAD7, CHMP4B**
Neurotrophin signaling pathway	**4,2358E-13**	**5**	**MAP3K3, NGFR, SHC1, PIK3R2, RELA, RPS6KA3, ARHGDIA, RAPGEF1, BAX, MAPK1, PLCG1**
Focal adhesion	6,05774E-13	4	LAMA5, SHC1, PIK3R2, ELK1, CCND1, MAPK1, VASP, GRLF1, VAV2, COL6A1, ITGA11, RAPGEF1
Proteoglycans in cancer	3,15804E-12	5	SDC4, PIK3R2, ELK1, CCND1, GPC1, MAPK1, PLCG1, VAV2, RPS6KB2, ARHGEF1, PTPN6, FGFR1
Glycerolipid metabolism	3,82705E-12	1	AGPAT1, AGPAT2, AGPAT4
SNARE interactions in vesicular transport	**6,46398E-12**	**3**	**VAMP2**
TNF signaling pathway	1,08568E-11	2	PIK3R2, TRAF2, RELA, RPS6KA4, CREB3L3, MAPK1, JUNB
Chronic myeloid leukemia	1,34911E-11	5	RB1, SHC1, PIK3R2, RELA, CCND1, E2F1, MAPK1
Fc gamma R-mediated phagocytosis	3,0438E-11	5	VASP, SPHK2, PIK3R2, DNM2, VAV2, MAPK1, PIP5K1A, PLCG1, WASF2
Hepatitis B	5,52921E-11	5	RB1, PIK3R2, ELK1, RELA, CCND1, YWHAQ, E2F1, BAX, MAPK1, PTK2B, FADD
Colorectal cancer	1,09676E-10	5	APC2, PIK3R2, AXIN2, CCND1, BAX, CYCS, MAPK1, RAC3, RALGDS
Apoptosis	**1,21339E-10**	**4**	**DFFA, PIK3R2, TRAF2, RELA, PRKAR2A, BAX, CYCS, CAPN1, FADD**
GnRH signaling pathway	1,58743E-10	3	MAP3K3, ELK1, PLCB3, GNA11, MAPK1, PTK2B
T cell receptor signaling pathway	1,69056E-10	5	PIK3R2, RELA, VAV2, MAPK1, PTPN6, PLCG1, NFKBIB
Adherens junction	1,88693E-10	5	MAPK1, RAC3, PTPN6, WASF2, FGFR1
Fat digestion and absorption	2,43063E-10	1	AGPAT1, AGPAT2
Synaptic vesicle cycle	**2,64159E-10**	**3**	**AP2A1, CPLX2, DNM1, VAMP2**
Epstein-Barr virus infection	3,38556E-10	5	PIK3R2, RELA, RELB, YWHAQ, POLR3H, TAB1
Transcriptional misregulation in cancer	4,4283E-10	3	MAX, MLLT1, RELA, CCND2, RXRG, NGFR, TAF15, JUP, FUS, TFE3, ETV4, RARA, TCF3
B cell receptor signaling pathway	6,64022E-10	5	INPPL1, PIK3R2, RELA, VAV2, CD79A, MAPK1, PTPN6, NFKBIB
ECM-receptor interaction	**6,76663E-10**	**2**	**LAMA5, COL6A2, COL6A1, ITGA11**
Ras signaling pathway	**7,02702E-10**	**4**	**SHC1, PIK3R2, ELK1, RELA, SYNGAP1, MAPK1, PLCG1, RALGDS, NGFR, EFNA3, RASA3, GNB1, EPHA2**
ErbB signaling pathway	**1,05542E-09**	**4**	**SHC1, PIK3R2, ELK1, RPS6KB2, MAPK1, PLCG1**

(*Continued*)

Table 5. (*Continued*)

Pathways	p-value	Occurrence	Affected Genes
Basal transcription factors	1,55859E-09	3	TAF6L, TAF15
Bladder cancer	3,01127E-09	5	RB1, CCND1, E2F1
Prostate cancer	4,59634E-09	5	RB1, PIK3R2, RELA, CCND1, E2F1, MAPK1, FGFR1
Non-small cell lung cancer	4,90448E-09	4	RB1, PIK3R2, RXRB, CCND1, E2F1, MAPK1, PLCG1, RXRG
Rap1 signaling pathway	7,80956E-09	5	VASP, NGFR, PIK3R2, ACTG1, VAV2, PLCB3, RAPGEF1, MAPK1, PLCG1, RALGDS, RAPGEF6, EPHA2, FGFR1
Viral carcinogenesis	7,87916E-09	5	RB1, PIK3R2, RELA, MAPK1, SCRIB, BAX
Regulation of actin cytoskeleton	**8,30967E-09**	**1**	**CYFIP2, GRLF1, PIK3R2, ACTN4, BAIAP2, FGD1, ACTG1, VAV2, ITGA11, MAPK1, PIP5K1A, ARHGEF1, WASF2, GIT1, FGFR1**
Small cell lung cancer	9,88309E-09	5	RB1, CCND1, E2F1, CYCS, TRAF2, RELA
Chemokine signaling pathway	1,00353E-08	5	SHC1, ARRB1, PIK3R2, ARRB2, RELA, VAV2, PLCB3, ADRBK1, GRK6, MAPK1
Acute myeloid leukemia	1,2986E-08	4	JUP, PIK3R2, RELA, CCND1, RPS6KB2, PIM1, RARA, MAPK1
Pancreatic cancer	2,24346E-08	5	RB1, PIK3R2, RELA, CCND1, E2F1, MAPK1, RAC3
Osteoclast differentiation	2,32427E-08	3	JUND, FHL2, PIK3R2, TRAF2, RELA, RELB, MAPK1, JUNB
Progesterone-mediated oocyte maturation	2,40544E-08	3	PIK3R2, PKMYT1, CDC25A, RPS6KA3, FZR1, MAPK1
Spliceosome	2,46814E-08	2	SF3A2, RBM8A, U2AF1, PRPF19, THOC4, U2AF2
Bacterial invasion of epithelial cells	2,49617E-08	4	SHC1, PIK3R2, DNM1, DNM2, WASF2
Fc epsilon RI signaling pathway	2,98389E-08	3	PIK3R2, VAV2, MAPK1, RAC3, PLCG1
Endometrial cancer	5,11242E-08	4	APC2, CCND1, MAPK1, PIK3R2, AXIN2, ELK1
Proteasome	5,88839E-08	2	
Wnt signaling pathway	**9,1423E-08**	**4**	**APC2, FBXW11, AXIN2, CSNK1E, CCND1, DVL2, RAC3**
Shigellosis	9,26388E-08	5	FBXW11, U2AF1, RELA, MAPK1, NFKBIB
Glioma	**1,00691E-07**	**4**	**RB1, SHC1, PIK3R2, CCND1, E2F1, MAPK1, PLCG1**
Notch signaling pathway	**1,15517E-07**	**3**	**APH1A, NCOR2, DVL2, DTX2**
Thyroid hormone signaling pathway	1,24296E-07	3	GATA4, PIK3R2, ATP1B1, RXRB, CCND1, MAPK1, PLCG1, RXRG
Hippo signaling pathway	**2,79196E-07**	**1**	**FBXW11, SCRIB, AXIN2, CSNK1E, SMAD7, CCND1, YWHAQ, DVL2**
Citrate cycle (TCA cycle)	2,98326E-07	1	OGDH
Renal cell carcinoma	3,93043E-07	3	RAPGEF1, ARNT, MAPK1, PIK3R2, VHL
AMPK signaling pathway	5,05726E-07	3	CRTC2, PIK3R2, CAMKK1, STK11, CCND1, FASN, HNF4A, AKT1S1, RPS6KB2

(*Continued*)

Table 5. (*Continued*)

Pathways	p-value	Occurrence	Affected Genes
Choline metabolism in cancer	7,23983E-07	4	PIK3R2, DGKZ, DGKQ, MAPK1, PIP5K1A, PLCG1, RALGDS, WASF2
Thyroid cancer	7,26445E-07	3	RET, RXRB, CCND1, MAPK1
Nucleotide excision repair	7,67343E-07	1	LIG1, POLE
Natural killer cell mediated cytotoxicity	1,04223E-06	3	FCER1G, SHC1, PIK3R2, VAV2, SH3BP2, MAPK1, PTK2B, PTPN6, PLCG1
Prolactin signaling pathway	1,11893E-06	3	SHC1, MAPK1, PIK3R2, RELA
Platelet activation	1,18344E-06	4	VASP, FCER1G, PIK3R2, ACTG1, PLCB3, MAPK1, ARHGEF1
Insulin signaling pathway	1,39589E-06	5	SHC1, INPPL1, PIK3R2, ELK1, RAPGEF1, MAPK1
mTOR signaling pathway	1,63553E-06	4	RPS6KA3, STK11, AKT1S1, RPS6KB2, MAPK1, PIK3R2
Vasopressin-regulated water reabsorption	1,80142E-06	1	RAB5C, VAMP2, RAB11B
Axon guidance	**2,29678E-06**	**2**	**SEMA4C, L1CAM, EFNA3, MAPK1, RAC3, EPHA2**
Oocyte meiosis	3,11271E-06	2	FBXW11, PKMYT1, YWHAQ, MAPK1
TGF-beta signaling pathway	3,8067E-06	3	MAPK1, SMAD6, SMAD7
Salmonella infection	3,87325E-06	2	PKN3, RELA, KLC3, KLC2, MAPK1
Estrogen signaling pathway	4,48771E-06	2	CALML5, SHC1, PIK3R2, CREB3L3, MAPK1
Amyotrophic lateral sclerosis (ALS)	**6,28617E-06**	**2**	**BAX, CYCS, NOS1**
Sphingolipid signaling pathway	6,6267E-06	4	FCER1G, SPHK2, PIK3R2, TRAF2, RELA, PPP2R2B, MAPK1
NF-kappa B signaling pathway	9,00498E-06	2	PIAS4, LRDD, RELA, RELB, LBP, PLCG1
HIF-1 signaling pathway	9,5515E-06	4	ARNT, PIK3R2, RELA, RPS6KB2, MAPK1, PLCG1, VHL
NOD-like receptor signaling pathway	1,02878E-05	1	MAPK1, RELA, NFKBIB
FoxO signaling pathway	1,05545E-05	3	PRMT1, PIK3R2, CSNK1E, STK11
Glutamatergic synapse	**1,12921E-05**	**1**	**GRIK5, GRIK3, PLCB3, GRM4, DLG4, ADRBK1, GNB1, MAPK1**
Endocrine and other factor-regulated calcium reabsorption	1,14065E-05	3	AP2A1, AP2B1, ATP1B1, AP2A2, DNM1, DNM2
Melanoma	1,15013E-05	2	RB1, CCND1, E2F1, MAPK1, PIK3R2
Pathogenic Escherichia coli infection	1,21309E-05	2	YWHAQ
Dopaminergic synapse	**1,70854E-05**	**1**	**CALML5, ARRB2, CREB3L3**
Epithelial cell signaling in Helicobacter pylori infection	1,88839E-05	1	CSK, GIT1, RELA
Type II diabetes mellitus	2,27294E-05	1	MAPK1, PIK3R2
Leukocyte transendothelial migration	2,50496E-05	3	VASP, GRLF1, PIK3R2, ACTN4, ACTG1, VAV2, PTK2B, PLCG1

(*Continued*)

Table 5. (*Continued*)

Pathways	p-value	Occurrence	Affected Genes
VEGF signaling pathway	3,35777E-05	1	SPHK2, MAPK1, PIK3R2
Ubiquitin mediated proteolysis	3,39334E-05	1	PIAS4, FBXW11, PRPF19, FZR1, VHL
Herpes simplex infection	3,52446E-05	1	RELA, PER1, TAF6L, CYCS, FADD, TAB1
Adipocytokine signaling pathway	3,84037E-05	2	RXRB, STK11, TRAF2, RXRG, CAMKK1, RELA, NFKBIB
Chagas disease (American trypanosomiasis)	5,31326E-05	1	PLCB3, PPP2R2B, GNA11, MAPK1, PIK3R2, FADD, RELA
Toxoplasmosis	5,53351E-05	1	RELA, CYCS, MAPK1, NFKBIB
HTLV-I infection	8,18359E-05	1	RB1, CRTC2, PIK3R2, IL2RG, ELK1, RELA, RELB, CCND1, DVL2, E2F1, APC2, EGR1, MAP3K3, BAX, TCF3
PI3K-Akt signaling pathway	**8,27352E-05**	**1**	**LAMA5, CRTC2, PIK3R2, IL2RG, RELA, STK11, CCND1, YWHAQ, MAPK1, NGFR, EFNA3, RPS6KB2, EPHA2**
p53 signaling pathway	**9,0672E-05**	**2**	**CCND2, CCND1, LRDD, BAI1**

doi:10.1371/journal.pone.0170585.t005

neural stem cell maintenance in the SVZ [58]. Thus, the fact that a significant number of genes regulated by Pea3 turn out to be immune system-related should be noted.

Verification of axon guidance pathway and related genes

It should be emphasized that KEGG Pathway database is a collection of manually drawn wiring diagrams for pathways and, while immensely informative, it unfortunately does not cover all genes involved in any particular pathway [61]. We have therefore gone back to the original microarray data in the light of PANOGA analysis, and compared genes identified in the significant pathways with the genes identified in the manually curated data. Some of the *in silico*-identified genes (Tables 3 and 4) were indeed found to be affected in microarray data, including L1CAM, NGFR, PTK2B and EFNB2, to be either up- or down-regulated; others, such as neuron-specific cyclin dependent kinase CDKR51 did not yield a statistically significant result, whereas its close homolog CDK5R2 was found to be repressed by around 2-fold in SH-SY5Y cells, and CDK10 was repressed by around 4-fold (data not shown). Based on these, we have restricted our verification analyses to potential novel targets of Pea3 that could be directly involved in axonal growth, guidance, and neural circuit formation that were common in all three analyses—manual curation, *in silico* automated analysis and microarray (data not shown). Among these are EFNA3, EFNB1, EFNB2, FGFR1, NGFR, PTK2B, SEMA4C, UNC5A, L1CAM, EPHA1, EPHA2, GLUD2 and GRIK3.

Using qRT-PCR assays in SH-SY5Y cells transfected with pCDNA3 or pCMV-mPea3-VP16 expression plasmids, we have first confirmed repression of EFNA3, EFNB1, EFNB2, FGFR1, NGFR, PTK2B, SEMA4C, UNC5A and L1CAM genes when Pea3-VP16 protein was overexpressed (Fig 2a). On the contrary, EPHA1, EPHA2, GLUD2 and GRIK3 were upregulated upon Pea3-VP16 expression (Fig 2b). The fold-changes between qRT-PCR and microarray assays were compared and found to be parallel to each other, ie repressed in both or activated in both, even though the extent of repression or activation may be different due to the resolution and sensitivity of the assay used (Fig 2c). When the promoters for these genes were analyzed for potential Pea3 binding motifs, some (but not all) of the negatively regulated gene promoters did not exhibit a high-affinity binding motif for Pea3, indicating at least some of

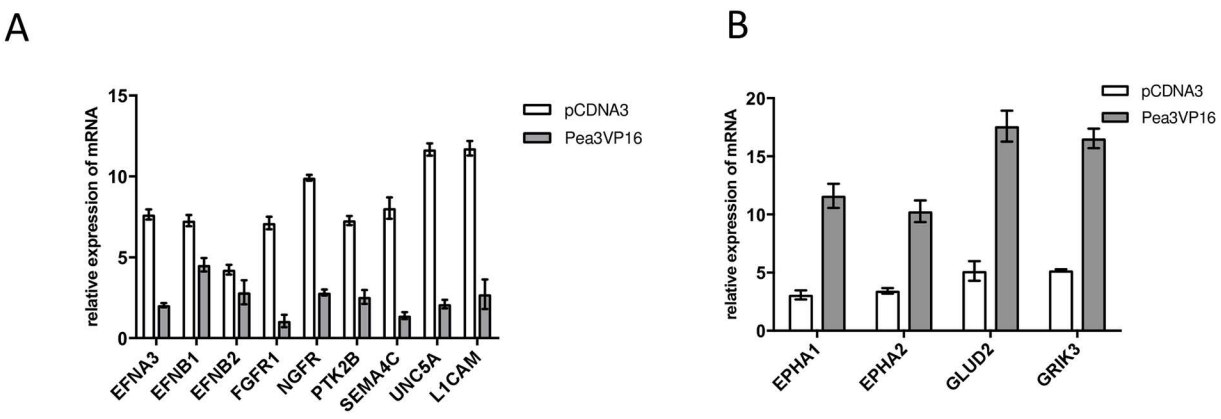

C

Gene ID	QPCR	Microarray	
	Fold change	Fold change	P value
EFNA3	-3,8	-5,3	0,00009
EFNB1	-2,7	-3,1	0,047
EFNB2	-2,6	-3,1	0,032
FGFR1	-6,7	-7	0,037
NGFR	-3,5	-8,5	0,001
PTK2B	-2,8	-2,7	0,012
SEMA4C	-5,7	-11,6	0,001
UNC5A	-5,5	-5,4	0,006
L1CAM	-4,3	-6	0,005
EPHA1	3,8	2,7	0,048
EPHA2	3	2,1	0,042
GLUD2	3,4	2,1	0,035
GRIK3	3,1	2,7	0,048

D

		# of motifs identified with dissimilarity scores:		
Gene ID	Promoter ID	0-1%	1-3%	3-5%
EFNA3	1318	0	0	0
EFNB1	43395, 116106	0	0	0
EFNB2	11194, 11195, 11196, 115856	0	0	0
FGFR1	41051, 122162, 122163	0	1	2
NGFR	17439, 17440, 17441, 114692	0	0	0
PTK2B	39829, 115864, 125599	0	0	0
SEMA4C	25323, 25326	0	0	2
UNC5A	33780	2	0	0
L1CAM	43934, 113184	0	0	1
EPHA1	116715	1	0	2
EPHA2	116108	0	0	1
GLUD2	N/A			
GRIK3	3628, 3629, 113464	0	1	1

Fig 2. Verification and analysis of a subset of target promoters. (a) q-RT-PCR results for a set of genes that were repressed upon Pea3-VP16 overexpression in SH-SY5Y cells (grey bars) as compared to pCDNA3-transfected cells (white bars); (b) q-RT-PCR results for a set of genes that were activated upon Pea3-VP16 overexpression in SH-SY5Y cells (grey bars) as compared to pCDNA3-transfected cells (white bars); (c) comparison of fold change in q-RT-PCR assay vs microarray results; (d) analysis of promoters for these genes for putative Pea3 binding sites, if available.

doi:10.1371/journal.pone.0170585.g002

the repression events may be indirect (Fig 2d; no promoter sequence was available for GLUD2 in the database utilized). Yet, high affinity Pea3 binding sites were predicted in some of the negatively regulated gene promoters, such as FGFR1 and Sema4C, and in some positively regulated gene promoters such as EPHA1 and EPHA2 (Fig 2d). Whether Pea3 can indeed bind to these predicted sites *in vivo* remains to be determined.

Kallikreins—novel Pea3 targets

A novel set of targets were also identified upon analysis of microarray data, which were not identified through *in silico* studies: kallikreins, serine proteases that cleave peptide bonds in proteins found in many physiological systems. Unlike matrix metalloproteases (MMPs), which are among the known targets of Pea3-dependent transcriptional regulation that degrade mainly extracellular matrix proteins, kallikreins have been implied in degradation of hormones such as somatostatin and pro-insulin (KLK1; [62]), myelin, amyloid peptide, GluR and α-synuclein (KLK6; [62]), L1-CAM (KLK8/neuropsin; [63, 64]), and ephrin-B2 (KLK4; [65]). Using qRT-PCR assays in SH-SY5Y cells transfected with pCDNA3 or pCMV-mPea3-VP16 expression plasmids, we have first confirmed transactivation results seen in microarray for

A

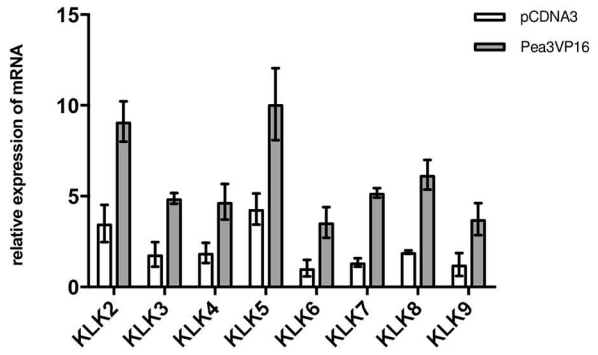

B

Gene ID	QPCR	Microarray	
	Fold change	Fold change	P value
KLK2	2,7	2,1	0,01
KLK3	3	2,7	0,042
KLK4	2,7	2	0,023
KLK5	2,5	2,7	0,008
KLK6	3,7	3,2	0,033
KLK7	3,8	2,8	0,007
KLK8	3,2	2,6	0,016
KLK9	3,8	2,3	0,042

C

		# of motifs identified with dissimilarity scores:		
Gene ID	Promoter ID	0-1%	1-3%	3-5%
KLK2	21177, 21178, 21179, 116944	0	0	7
KLK3	21173, 21174, 21175, 21176, 112536, 31945	0	1	5
KLK4	116479, 21684	1	0	2
KLK5	118481	0	0	1
KLK6	114901, 21679	0	1	1
KLK7	21677, 116571	2	0	0
KLK8 (mouse)	76582	1	0	1
KLK9	118135	1	0	0

Fig 3. Analysis of kallikreins as novel targets for Pea3. (a) q-RT-PCR results for KLK2-9 that were activated upon Pea3-VP16 overexpression in SH-SY5Y cells (grey bars) as compared to pCDNA3-transfected cells (white bars); (b) comparison of fold change in q-RT-PCR assay vs microarray results; (d) analysis of kallikrein promoters for putative Pea3 binding sites.

doi:10.1371/journal.pone.0170585.g003

KLK2-9 (Fig 3a). When the fold-activations in qRT-PCR assays were compared to those observed in microarray experiment, they were found to be consistently activated between 2- to 4-fold (Fig 3b). When the promoters of these genes were analyzed, all of them were predicted to contain one or more putative Pea3 binding motifs that exhibit 0–5% dissimilarity (Fig 3c). KLK2 and KLK3, which are largely studied with respect to prostate cancer (Lisle et al, 2015) showed large number of relatively low-affinity Pea3 motifs, whereas KLK6 and KLK8, shown to cleave α-synuclein and L1-CAM, respectively, had higher-affinity binding motifs (Fig 3c). Whether Pea3 directly binds to and regulates these promoters in neurons remain to be studied, however it should be noted that KLK8, for example, was shown to induce neurite growth and fasciculation of hippocampal neurons as well as formation and maturation of synaptic boutons in Schaffer collateral pathways, and to regulate Schaffer collateral long term potentiation (LTP) in hippocampus [63–68], suggesting kallikreins, particularly KLK6 and KLK8, as novel transcriptional targets of Pea3.

Binding of Pea3 on promoters

One rather interesting and surprising result of microarray experiments that could not be foreseen through *in silico* analyses was the large set of genes that were repressed upon Pea3-VP16 overexpression in SH-SY5Y cells (data not shown). Some of the repression events were then confirmed through qRT-PCR (Fig 2). One explanation could be the switch of Pea3 ETS protein

from an activator to a repressor through SUMOylation [69–71]. However, since VP16 is a highly potent transactivator, the repression observed was thought to be through an indirect mechanism, where Pea3-VP16 activates a global repressor or a miRNA gene. This is a likely mechanism, because the promoters of some of the repressed genes analyzed exhibited no high-affinity binding sites for Pea3 (Fig 2d).

To confirm whether Pea3 can directly or indirectly bind to the identified subset of promoters, we have conducted chromatin immunoprecipitation (ChIP) assays on some of the *ets* motifs identified through *in silico* promoter analyses (Fig 2d). Indeed, Pea3-VP16 was found to bind both *epha1* and *ehpa2* promoters, albeit with different intensities on different *ets* motifs (Fig 4a). *Epha1* promoter was found to have one *ets* motif with dissimilarity score (ds) smaller than 1% (ds 0.60%), and two *ets* motifs with dissimilarity scores between 3 and 5% (Fig 2d). Pea3-VP16 showed higher binding to the former motif (epha1 2), and lower binding to the latter two (epha1 1 and epha1 3), as expected from *in silico* prediction (Fig 4a). *Epha2* promoter had slightly lower binding of Pea3-VP16 to the epha2 1 motif, which in fact contains two tandem *ets* motifs with relatively high dissimilarities (ds 7.42%, shown in Fig 4a, and ds 10.54%, not shown); epha 2 2 motif has a higher ds score than epha2 1, reflected in ChIP assay; Fig 4a).

Similarly, *l1cam* and *sema4c* promoters were also confirmed to bind Pea3-VP16, in spite of the fact that *ets* motifs of both promoters show high dissimilarity rates (Figs 2d and 4a; ds 4.31%). *Akt* promoter contained two *ets* motifs, one of which showed a stronger binding to Pea3-VP16 in ChIP assays (Fig 4a; ds 6.82%), and the stronger *ets* motif of *fgfr1* promoter also indicated Pea3-VP16 binding (ds not shown) Other target promoters from different KEGG pathways were also found to give higher qPCR results in ChIP assays, such as *cxcr4*, *rhoA* and *elk-1* promoters (data not shown). *Mmp9* promoter was used as a positive control for Pea3 binding (ds 0%, Fig 4a [72]).

We have then analyzed promoter regions for up- or down-regulated genes for putative Pea3 binding motifs, and analyzed these sites using WebLogo tool for common patterns. When promoters of genes that were up- or down-regulated 2- to 5-fold were separately analyzed, the classical GGA core motif [2,73] was observed in both groups (TCCT/AGGA; summarized in Fig 4b). These motifs were also confirmed in the limited ChIP assays (Fig 4a). However, when promoters of genes downregulated 5-fold or more were grouped and analyzed separately, the putative Pea3 binding motifs predicted, if any, were quite far from the consensus 5'-AGGAAG-3' binding site ([2]; ACGT/TGCA; data not shown), indicating an indirect repression mechanism by Pea3 (see Conclusion).

Conclusion

ETS transcription factors were shown to be regulated in a temporally regulated manner at later stages of nervous system development, in particular for normal sensory neuron differentiation and during branching [74]. Pea3 family of proteins are expressed from E9.5 till birth, and in some cases after birth, starting with brain regions followed by expression in lung, thymus, cartilage and mammary tissue of mouse [75]. Pea3 and Er81 appear to be particularly important at later stages of neural development, whereas Erm seems to be involved in early differentiation of neural crest stem cells [76].

Glial-derived neurotrophic factor (GDNF) as well as Met signaling were shown to regulate the expression of Pea3 proteins in prospective motor neurons, and in a mutually exclusive manner in subpopulations of motor neuron pools [77–79]. Fibroblast growth factors (FGFs) were also shown to regulate Pea3 subfamily members during development at various brain regions and retina [15, 80]. In the retina, FGF was shown to regulate Pea3 expression in a MAPK-dependent manner, resulting in expression of neurofilament-M, which was also

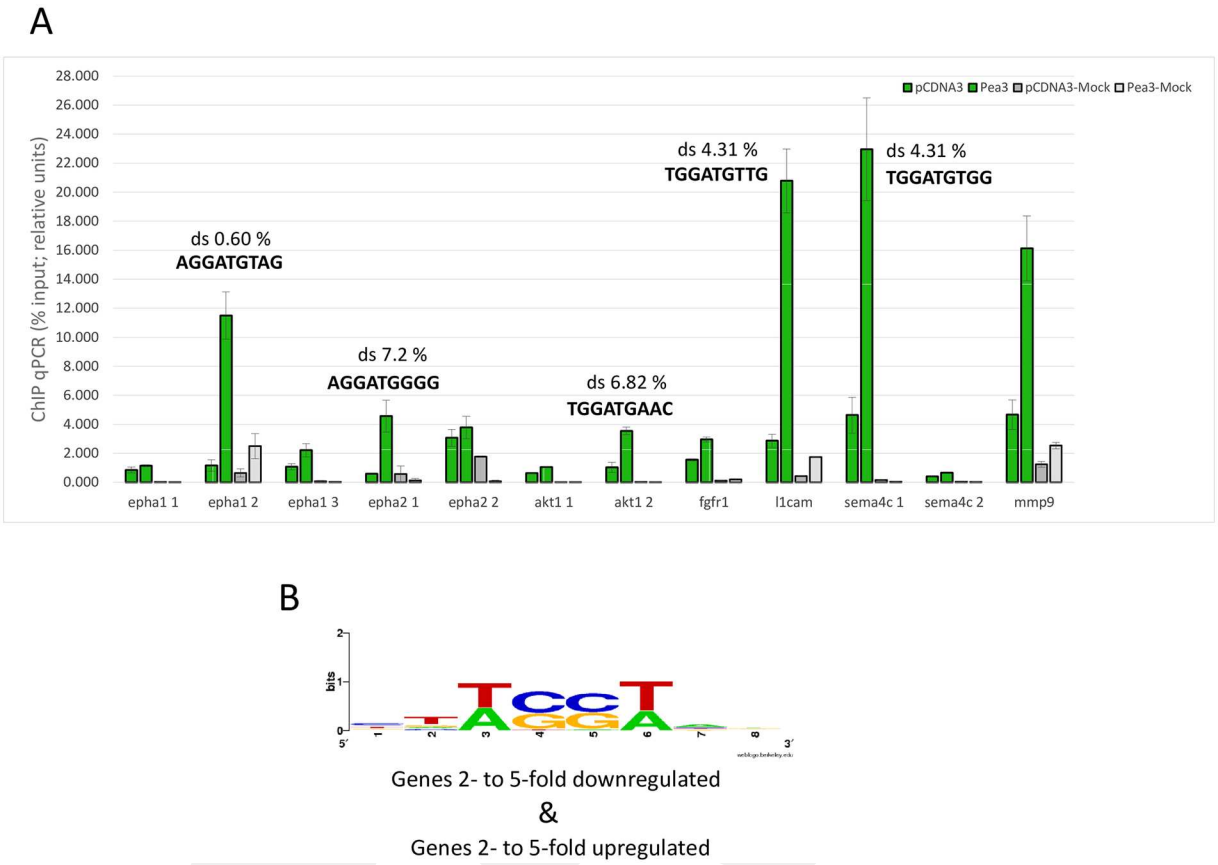

Fig 4. Chromatin immunoprecipitation (ChIP) and Pea3-VP16 binding. (a) ChIP PCR in untransfected vs Pea3-VP16 overexpressing SH-SY5Y cells, immunoprecipitated with either Flag antibody (Flag IP) or IgG (IgG IP). Dissimilarity score (ds) of selected *ets* motifs are indicated, and explained further in text; (b) weblogo analysis for genes that were either 2- to 5-fold downregulated or2- to 5-fold upregulated upon Pea3-VP16 expression in SH-SY5Y cells.

doi:10.1371/journal.pone.0170585.g004

confirmed to be a Pea3 target by our laboratory [6, 7, 15]. In the chick, FGF3-dependent upregulation of Pea3 was shown to be important for Krox20-dependent hindbrain segmentation [81]. It should be noted that no significant change in Krox20/EGR2 was observed in our microarray analysis, whereas a repression of around 7-fold was seen on EGR1 levels (data not shown).

In spite of many reports on the role and importance of Pea3 subfamily members in nervous system development, only cadherin-8, Ephrin receptor 4 (Ephr4), semaphorin-3E and neurofilaments were previously shown to be targets of Pea3 [7, 16, 18]. In *C. elegans*, ETS protein Ast-1 (axon steering defect-1) was shown to be responsible for dopaminergic neuron differentiation, with loss of *ast-1* causing the failure of all dopaminergic neurons to terminally differentiate [17]. In this system, Ast-1 was shown to regulate major dopaminergic pathway genes through a dopamine (DA) motif, although a counterpart function for Pea3 subfamily member Er81/ETV1 is not yet confirmed for mammalian dopaminergic system [17].

In this study, we have developed an automated tool for identification of potential novel target promoters for regulation by given transcription factors, which we have used to identify novel Pea3 target genes; the analysis was further supported by microarray studies. Our results indicate that such *in silico* tools can indeed identify genuine binding sites with significant accuracy, yet fail to indicate whether such a binding would result in activation or repression. In the

microarray analysis presented in this study, we have identified novel targets of Pea3 transcription factor that are both down- and up-regulated. Our chromatin immunoprecipitation studies analyzed direct binding of Pea3 to a small subset of promoters, and parallel q-RT-PCR assays confirmed some of the repressions observed in microarray experiments (Figs 2 and 4). Earlier studies indicate that, while mostly known as transactivators, ETS proteins can act as repressors depending on post-translational modification status, such as SUMOylation [71]. Therefore, such post-translational modifications on Pea3 fusion partner of Pea3-VP16 protein may also affect transcriptional regulation of target promoters. Additionally, binding of Pea3-VP16 to these promoters may be sterically hindering a crucial transactivator from binding, thereby causing a repression of a subset of genes outside a rather narrow developmental window, ensuring timely expression of such critical genes. Another explanation could be post-translational modifications of Pea3, since similar modifications such as SUMOylation have been known to convert some ETS family members to repressors [69–71].

In addition to components of Wnt, Notch and Hippo pathways, genes within Endocytosis, Synaptic vesicle cycling and Immune pathways were also found to be potential targets of Pea3 in microarray analysis (Table 5). Extensive analysis is required to further illuminate the mechanism and relevance of these potential targets for neural circuit formation.

In line with a relatively late-stage function of Pea3 in nervous system development, it appears that genes related to axonal guidance or axon-axon interaction are down-regulated, directly or indirectly, whereas genes related to survival, neurite outgrowth and maturation of synaptic boutons, as well as neural activity were upregulated (Fig 5). While Sema4C is downregulated (Fig 2a and 2c), plexin A1, a co-receptor for semaphorins, is also downregulated (around 5-fold; data not shown). Among the genes identified in microarray experiments, EFNA3, for example, was shown to be expressed in primitive streak in early mouse embryos [46], and EFNB2 plays a role in early cortical development [48], both of which are down-regulated upon Pea3-VP16 expression in microarray and qRT-PCR studies (Fig 2a and 2c), whereas EPHA1 and EPHA2, involved in neurite outgrowth and post-natal neuromuscular junction formation [82] are up-regulated (Fig 2b and 2c). These data support earlier reports that Pea3 family members were functional at late stages of neuronal circuit formation [83]. Having said that, the story of ephrins and ephrin receptors in neurons appears to be more complicated—for example, EphB2, the receptor for ephrin B, is important for synaptic signaling and LTP formation [82] and EPHA2 was shown to be important in mammalian neural precursor cell (NPC) differentiation and neurogenesis [45], yet EFNB1 and EphA2 together were found to play a role in neurite outgrowth. EFNB2 on the membranes of vascular endothelial cells, on the other hand, blocks cell cycle entry in order to maintain stem cell identity [84]. Hence, more in-depth analysis of how different Pea3 family members dynamically regulate different ephrins and ephrin receptors in a spatiotemporal manner is required.

Nonetheless, it is intriguing that kallikrein KLK8 is upregulated upon Pea3 expression, while at the same time its substrate L1CAM is downregulated (Figs 2, 3 and 5). Similarly, as KLK4 was upregulated, its substrate EFNB2 was downregulated by Pea3 (Figs 2, 3 and 5). No such parallels were found between KLK6, which was upregulated (Figs 3 and 5), and its substrates APP (no significant change; data not shown) or a-synuclein (no significant change; data not shown). One of the predicted KLK6 substrates is glutamate receptor GluR [62], yet excitatory ionotropic glutamate receptor GRIK3 (otherwise known as GluR7) was upregulated nearly 3-fold (Fig 2b and 2c), and metabotropic glutamate receptor GRM4 was upregulated around 2.5-fold (data not shown). Why both the enzyme and its substrates are up-regulated at the same time is yet unclear, however the fact that many other excitatory ion channels such as nicotinic cholinergic receptor CHRNA2 is upregulated by around 2.5-fold, while inhibitory chloride channel CLCN7 was downregulated by around 12-fold (data not shown) indicates an

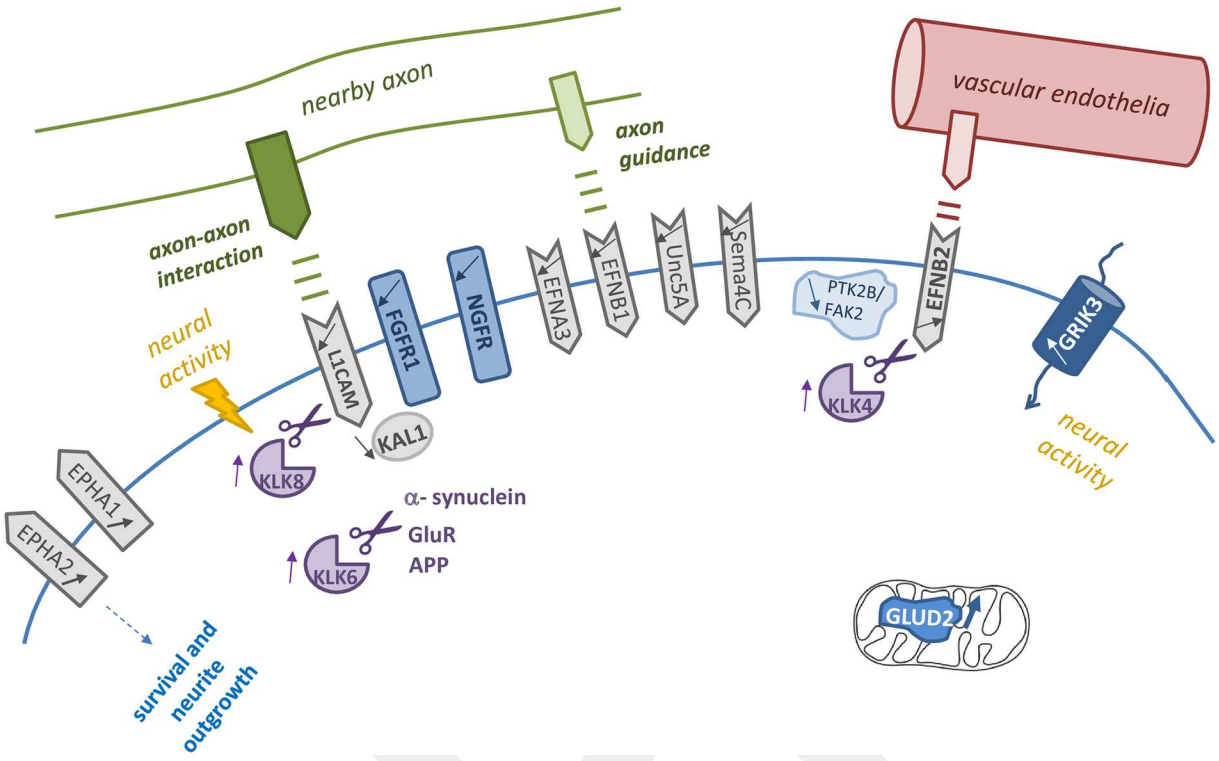

Fig 5. A schematic summary of genes that were identified to be novel targets for Pea3 analyzed in this study, along with their interactions and functions; L1CAM, EFNA3, EFNB1, Unc5A and SEMA4c are involved in axon-axon interactions and axonal guidance; KLK8 activated by neural activity was shown to degrade L1CAM, and KLK4 was reported to cut EFNB2, while KLK6 was shown to cleave α-synuclein, GluR and APP. EFNB2 on vascular endothelial cells helps maintain stem cell identity. FGFR1 and its partner KAL1, involved in post-mitotic development of neuronal cells, are both downregulated. EPHA1 and EPHA2, both upregulated, are involved in survival and neurite outgrowth. GLUD2 and GRIK3, both correlated with neuronal activity, are upregulated in Pea3-VP16-expressing cells.

doi:10.1371/journal.pone.0170585.g005

active role for Pea3 in neuronal activity upon terminal differentiation. Also upregulated are genes involved in synaptic vesicles, such as synaptotagmin (2.8-fold), those involved in neurotransmitter release, such as DOC2A (2.5-fold), and myelination, such as myelin oligodendrocyte glycoprotein (MOG, 2.5-fold) (data not shown). Some of the genes identified in this study can also explain the involvement of Pea3 family members in many forms of cancer. KLK2, 3, and 5 have all been implicated in prostate cancer, whereas KLK9 is implicated in both prostate and breast cancers, where Pea3 has been associated with [4, 13, 41]. Therefore we believe that this combinatorial approach to identifying novel targets of Pea3 not only will help us understand its role in nervous system, but also in progression of many types of cancer.

We would also like to emphasize that experimental as well as *in silico* assays and different algorithms such as that presented in this study could be used complementary to genome-wide microarray analyses so as to narrow down target identification and eliminate possible false negatives or wrong identifications.

Acknowledgments

We would like to acknowledge TUBITAK BIDEB project grants to UD and BE, as well as TUBITAK grants no 107S064 and 214Z278. We would also like to acknowledge GENMAR and SEMBIO companies as well as Nogayhan Seymen, Ali Kaynar and Ceyhun Erturk for their excellent assistance and consultation with microarray analysis, and also give our special

thanks to undergraduate project students Elif Yavaş, Ekin Sönmez, Yeşeren Kayacan and M. Soner Turkoner for their help with promoter analyses.

Author contributions

Conceptualization: IAK US UD BK.

Data curation: IAK US.

Formal analysis: UD BE ES BK BBG IMD.

Funding acquisition: IAK UD BE.

Investigation: BK UD.

Methodology: IMD BBG US.

Writing – original draft: IAK BK BBG US.

Writing – review & editing: BBG BK UD US IAK.

References

1. Graves BJ, Petersen JM. Specificity within the ETS family of transcription factors, Adv Cancer Res. 1998; 75: 1–55. PMID: 9709806
2. Xin JH, Cowie A, Lachance P, Hassell JA. Molecular cloning and characterization of PEA3, a new member of the Ets oncogene family that is differentially expressed in mouse embryonic cells. Genes Dev. 1992; 6:481–496 PMID: 1547944
3. Janknecht R. Analysis of the ERK-stimulated ETS-transcription factor ER81, Mol. Cell. Biol. 1996; 16: 1550–1556. PMID: 8657129
4. Trimble MS, Xin JH, Guy CT, Muller WJ, Hassell JA. PEA3 is overexpressed in mouse metastatic mammary adenocarcinomas. Oncogene 1993; 8: 3037–3042. PMID: 7692372
5. Vrieselling E, Arber S. Target induced transcriptional control of dendritic patterning and connectivity in motor neurons by the ETS gene Pea3. Cell 2006; 127: 1439–1452 doi: 10.1016/j.cell.2006.10.042 PMID: 17190606
6. Caglayan B, Savasan M, Erdogan B, Aksan IK. Pea3 transcription factor regulates axonal outgrowth: novel target genes. J Neurochem. 2010; 115(1): 16.
7. Kandemir B, Caglayan B, Hausott B, Erdogan B, Dag U, Demir O et al. Pea3 transcription factor promotes neurite outgrowth. Front. Cell. Neurosci. 2014; 7(59):1–11
8. Qin L, Liao L, Redmond A, Young L, Yuan Y, Chen H et al. The AIB1 oncogene promotes breast cancer metastasis by activation of PEA3-mediated matrix metalloproteinase 2 (MMP2) and MMP9 expression. Mol Cell Biol. 2008; 28(19): 5937–5950. doi: 10.1128/MCB.00579-08 PMID: 18644862
9. Chen JH, Vercamer C, Li Z, Paulin D, Vandenbunder B, Stehelin D. Pea3 transactivates vimentin promoter in mammary epithelial and tumor cells. Oncogene 1996; 13(8): 1667–1675. PMID: 8895512
10. de Launoit Y, Audette M, Pelczar H, Plaza S, Baert JL. The transcription of the intracellular adhesion molecule-1 is regulated by Ets transcription factors. Oncogene 1998; 16(16): 2065–2073. doi: 10.1038/sj.onc.1201726 PMID: 9572487
11. de Launoit Y, Chotteau-Lelievre A, Beaudoin C, Coutte L, Netzer S, Brenner C et al. The Pea3 group of ETS-related transcription factors: Role in breast cancer metastasis. Adv Exp Med Biol. 2000; 480: 107–116. doi: 10.1007/0-306-46832-8_13 PMID: 10959416
12. El-Tanani M, Platt-Higgins A, Rudland PS, Campbell FC. Ets gene Pea3 cooperates with beta-catenin-Lef-1 and c-Jun in regulation of osteopontin transcription. J Biol Chem. 2004; 279(20): 20794–20806. doi: 10.1074/jbc.M311131200 PMID: 14990565
13. Hua D, Chen B, Bai M, Yu H, Wu X, Jin W. PEA3 activates VEGF transcription in T47D and SKBR3 breast cancer cells. Acta Biochim Biophys. 2009; 41: 63–68.
14. Chotteau-Lelievre A, Dolle P, Peronne V, Coutte L, de Launoit Y, Desbiens X. Expression patterns of Ets transcription factors from the PEA3 group during early stages of mouse development. Mech Dev. 2001; 108(1–2): 191–195. PMID: 11578874

15. McCabe KL, McGuire C, Reh TA. Pea3 expression is regulated by FGF signaling in developing retina. Dev Dyn. 2006; 235: 327–335. doi: 10.1002/dvdy.20631 PMID: 16273524

16. Livet J, Sigrist M, Stroebel S, De Paola V, Price SR, Henderson CE et al. ETS gene Pea3 controls the central position and terminal arborization of specific motor neuron pools. Neuron 2002; 35(5): 877–892. PMID: 12372283

17. Flames N, Hobert O. Gene regulatory logic of dopamine neuron differentiation. Nature 2009; 458: 885–889. doi: 10.1038/nature07929 PMID: 19287374

18. Koo SJ, Pfaff SL. Fine-tuning motor neuron properties: signaling from the periphery. Neuron 2002; 35 (5): 823–826. PMID: 12372278

19. Zhao F, Xuan Z, Liu L, Zhang MQ. TRED: a Transcriptional Regulatory Element Database and a platform for in silico gene regulation studies. Nuc Acids Res. 2005; 33: D103–D107.

20. Farre D, Roset R, Huerta M, Adsuara JE, Rosello L, Alba MM et al. Identification of patterns in biological sequences at the ALGGEN server: PROMO and MALGEN. Nuc Acids Res. 2003; 31: 3651–3653.

21. Zhang X, Zhang B, Gao J, Wang X, Liu Z. Regulation of the microRNA 200b (miRNA-200b) by transcriptional regulators PEA3 and ELK-1 protein affects expression of the Pin1 protein to control anoikis. J Biol Chem. 2013; 288: 32742–32752. doi: 10.1074/jbc.M113.478016 PMID: 24072701

22. Higashino F, Yoshida K, Noumi T, Seiki M, Fujinaga K. Ets-related protein E1A-Fcan activate three different matrix metalloproteinase gene promoters. Oncogene 1995; 10: 1461–1463. PMID: 7731700

23. Crawford HC, Fingleton B, Gustavson MD, Kurpios N, Wagenaar RA, Hassell JA et al. The PEA3 subfamily of Ets transcription factors synergizes with beta catenin-LEF-1 to activate matrilysin transcription in intestinal tumors. Mol Cell Biol. 2001; 21(4): 1370–1383. doi: 10.1128/MCB.21.4.1370-1383.2001 PMID: 11158322

24. Durinck S, Moreau Y, Kasprzyk A, Davis S, De Moor B, Brazma A et al. BioMart and Bioconductor: a powerful link between biological databases and microarray data analysis. Bioinformatics 2005; 21: 3439–3440. doi: 10.1093/bioinformatics/bti525 PMID: 16082012

25. Durinck S, Spellman P, Birney E and Huber W. Mapping identifiers for the integration of genomic datasets with the R/Bioconductor package biomaRt. Nat Prot. 2009; 4: 1184–1191.

26. Shannon P. MotifDb: An Annotated Collection of Protein-DNA Binding Sequence Motifs. R package version 1.10.0; 2014.

27. Meydan C, Otu HH, Sezerman OU. Prediction of peptides binding to MHC class I and II alleles by temporal motif mining. BMC Bioinf. 2013; 14(Suppl 2): S13;

28. Pawitan Y, Michiels S, Koscielny S, Gusnanto A, Ploner A. False discovery rate, sensitivity and sample size for microarray studies. Bioinformatis 2005; 21(13): 3017–3024.

29. Xu Y, Li WL, Fu L, Gu F, Ma YJ. Slit2/Robo1 signaling in glioma migration and invasion. Neurosci Bull. 2010; 26(6): 474–478. PMID: 21113198

30. Chedotal A. Slits and their receptors. Adv Exp Med Biol. 2007; 621: 65–80. doi: 10.1007/978-0-387-76715-4_5 PMID: 18269211

31. Liao WX, Wing DA, Geng JG, Chen DB. Perspectives of Slit/Robo signaling in placental angiogenesis. Histol Histopathol. 2010; 25(9): 1181–1190. PMID: 20607660

32. Chaturvedi S, Robinson LA. Slit2-Robo signaling in inflammation and kidney injury. Pediatr Nephrol. 2015; 30(4): 561–566. doi: 10.1007/s00467-014-2825-4 PMID: 24777535

33. Dong Y, Harrington BS, Adams MN, Wortmann A, Stephenson SA, Lisle J et al. Activation of membrane-bound proteins and receptor systems: a link between tissue kallikrein and the KLK-related peptidases. Biol Chem. 2014; 395(9): 977–990. doi: 10.1515/hsz-2014-0147 PMID: 24854540

34. Diaz-Balzac CA, Lazaro-Pena MI, Ramos-Ortiz GA, Bulow HE. The adhesion molecule KAL-1/anosmin-1 regulates neurite branching through a SAX7/L1CAM-EGL-15/FGFR Receptor complex. Cell Rep. 2015; 11(9): 1377–1384. doi: 10.1016/j.celrep.2015.04.057 PMID: 26004184

35. Park I, Lee HS. EphB/ephrinB signaling in cell adhesion and migration. Mol Cells 2015; 38(1): 14–19. doi: 10.14348/molcells.2015.2116 PMID: 25475547

36. Day BW, Stringer BW, Boyd AW. Eph receptors as therapeutic targets in glioblastoma. Br J Cancer 2014; 111(7): 1255–1261. doi: 10.1038/bjc.2014.73 PMID: 25144626

37. Valable S, Bellail A, Lesne S, Liot G, Mackenzie ET, Vivien D et al. Angiopoietin-1-induced PI3-kinase activation prevents neuronal apoptosis. FASEB J. 2003; 17(3): 443–445. doi: 10.1096/fj.02-0372fje PMID: 12514118

38. Fuhrmann M, Bittner T, Jung CKE, Burgold S, Page RM, Mitteregger G et al. Microglial Cxc3r1 knockout prevents neuron loss in a mouse model of Alzheimer's disease. Nat Neurosci. 2010; 13: 411–413. doi: 10.1038/nn.2511 PMID: 20305648

39. Gary DS, Milhavet O, Camandola S, Mattson MP. Essential role for integrin linked kinase in Akt-mediated survival signaling in hippocampal neurons. J Neurochem. 2003; 84(4): 878–890. PMID: 12562530

40. Garcia-Garcia E, Pino-Barrio MJ, Lopez-Medina L, Martinez-Serrano A. Intermediate progenitors are increased by lengthening of the cell cycle through calcium signaling and p53 expression in human neural progenitors. Mol Biol Cell. 2012; 23 1167–1180. doi: 10.1091/mbc.E11-06-0524 PMID: 22323293

41. Qin J, Mizuguchi M, Itoh M, Takashima S. A novel migration-related gene product, doublecortin, in neuronal migration disorder of fetuses and infants with Zellweger syndrome. Acta Neuropathol. 2000; 100(2): 168–173 PMID: 10963364

42. Saito A, Miyajima K, Akatsuka J, Kondo H, Mashiko T, Kiuchi T et al. CaMKIIbeta-mediated LIM kinase activation plays a crucial role in BDNF-induced neuritogenesis. Genes Cells 2013; 18(7): 533–543. doi: 10.1111/gtc.12054 PMID: 23600483

43. Hayano Y, Sasaki K, Ohmura N, Takemoto M, Maeda Y, Yamashita T et al. Netrin-4 regulates thalamocortical axon branching in an activity-dependent fashion. Proc Natl Acad Sci USA. 2014; 111(42): 15226–15231. doi: 10.1073/pnas.1402095111 PMID: 25288737

44. Abdul-Aziz NM, Turmaine M, Greene ND, Copp AJ. EphrinA-EphA receptor interactions in mouse spinal neurulation: implications for neural fold fusion. Int J Dev Biol. 2009; 53: 559–568 doi: 10.1387/ijdb.082777na PMID: 19247962

45. Aoki M, Yamashita T, Tohyama M. EphA receptors direct the differentiation of mammalian neural precursor cells through a mitogen-activated protein kinase-dependent pathway. J Biol Chem. 2004; 279 (31): 32643–32650. doi: 10.1074/jbc.M313247200 PMID: 15145949

46. Duffy SL, Steiner KA, Tam PP, Boyd AW. Expression analysis of the Epha1 receptor tyrosine kinase and its high affinity ligands Efna1 and Efna3 during early mouse development. Gene Expr Patterns 2006; 6(7): 719–723. doi: 10.1016/j.modgep.2005.12.007 PMID: 16466970

47. Moscoso LM, Sanes JR. Expression of four immunoglobulin superfamily adhesion molecules (L1, Nr-CAM/Bravo, neurofascin/ABGP, and N-CAM) in the developing mouse spinal cord. J Comp Neurol. 1995; 352: 321–334 doi: 10.1002/cne.903520302 PMID: 7706555

48. North HA, Clifford MA, Donoghue MJ. Til Eph do us part': intercellular signaling via Eph receptors and ephrin ligands guides cerebral cortical development from birth through maturation. Cereb Cortex 2013; 23(8): 1765–1773. doi: 10.1093/cercor/bhs183 PMID: 22744705

49. Zou Y, Engert F, Tao HW. The assembly of neural circuits. Neuron 2004; 43: 159–163. doi: 10.1016/j.neuron.2004.07.004 PMID: 15260951

50. Zou Y. Wnt signaling in axon guidance. Trends in Neurosci. 2004; 27(9): 528–532.

51. Killeen MT, Sybingco SS. Netrin, Slit and Wnt receptors allow axons to choose the axis of migration. Dev Biol. 2008; 323: 143–151. doi: 10.1016/j.ydbio.2008.08.027 PMID: 18801355

52. Giniger E. Notch signaling and neural connectivity. Curr Opin Genet Dev. 2012; 22(4): 339–346. doi: 10.1016/j.gde.2012.04.003 PMID: 22608692

53. Redmond L, Ghosh A. The role of Notch and Rhoa GTPase signaling in the control of dendritic development. Curr Opin Neurobiol. 2001; 11: 111–117. PMID: 11179880

54. Shi M, Liu Z, Yonggang Lv, Zheng M, Du F, Zhao G et al. Forced Notch signaling inhibits commissural axon outgrowth in the developing chick central nerve system. PLoS One 2011; 6(1): e14570. doi: 10.1371/journal.pone.0014570 PMID: 21283742

55. Moleirinhi S, Patrick C, Tilston-Lunel AM, Higginson JR, Angus L, Antkowiak M et al. Willin, an upstream component of the Hippo signaling pathway, orchestrates mammalian peripheral nerve fibroblasts. PLoS One 2013; 8(4): e60028. doi: 10.1371/journal.pone.0060028 PMID: 23593160

56. Kim M, Jho EH. Cross-talk between Wnt/b-catenin and Hippo signaling pathways: a brief review. BMB Rep. 2014; 47(10): 540–545. doi: 10.5483/BMBRep.2014.47.10.177 PMID: 25154721

57. Jukam D, Xie B, Rister J, Terrell D, Charlton-Perkins M, Pistillo D et al. Opposite feedbacks in the Hippo pathway for growth control and neural fate. Science 2013; 342: 1238016–1 to -8.

58. Ziv Y, Schwartz M. Orchestrating brain-cell renewal: the role of immune cells in adult neurogenesis in health and disease. Trends Molec Med. 2008; 14(11): 471–478.

59. Doty KR, Guillot-Sestier MV, Town T. The role of the immune system in neurodegenerative disorders: adaptive or maladaptive? Brain Res. 2015; 1617: 155–173. doi: 10.1016/j.brainres.2014.09.008 PMID: 25218556

60. Neumann H, Schweigreiter R, Yamashita T, Rosenkranz K, Wekerle H, Barde Y-A. TNF inhibits neurite outgrowth and branching of hippocampal neurons by a Rho-dependent mechanism. J Neurosci. 2002; 22(3): 854–862. PMID: 11826115

61. Ogata H, Goto S, Sato K, Fujibuchi W, Bono H, Kanehisa M. KEGG: Kyoto Encyclopedia of Genes and Genomes. Nuc Acids Res. 1999; 27(1): 29–34.

62. Li HX, Hwang BY, Laxmikanthan G, Blaber SI, Blaber M, Golubkov PA et al. Substrate specificity of human kallikreins 1 and 6 determined by phage display. Protein Sci. 2008; 17(4): 664–672. doi: 10.1110/ps.073333208 PMID: 18359858

63. Matsumoto-Miyai K, Ninomiya A, Yamasaki H, Tamura H, Nakamura Y, Shiosaka S. NMDA-dependent proteolysis of presynaptic adhesion molecule L1 in the hippocampus by neuropsin. J Neurosci. 2003; 23(21): 7727–7736. PMID: 12944500

64. Konar A, Thakur MK. Neuropsin is associated with MAP2c dependent dendritic morphology in aging brain. Ther Targets Neurol Dis. 2015; 2:e503

65. Lisle JE, Mertens-Walker I, Stephens CR, Stansfield SH, Clements JA, Herington AC et al. Murine, but not human, ephrin-B2 can be efficiently cleaved by the serine protease kallikrein-4: implications for xenograft models of human prostate cancer. Exp Cell Res. 2015; 333(1): 136–146. doi: 10.1016/j.yexcr.2015.02.014 PMID: 25724897

66. Ishikawa Y, Horii Y, Tamura H, Shiosaka S. Neuropsin (KLK8)-dependent and—independent synaptic tagging in the Schaffer-collateral pathway of mouse hippocampus. J Neurosci. 2008; 28(4): 843–849. doi: 10.1523/JNEUROSCI.4397-07.2008 PMID: 18216192

67. Ishikawa Y, Tamura H, Shiosaka S. Diversity of neuropsin (KLK8)-dependent synaptic associativity in the hippocampal pyramidal neuron. J Physiol. 2011; 589(Pt 14): 3559–3573. doi: 10.1113/jphysiol.2011.206169 PMID: 21646406

68. Oka T, Akisada M, Okabe A, Sakurai K, Shiosaka S, Kato K. Extracellular serine protease neuropsin (KLK8) modulates neurite outgrowth and fasciculation of mouse hippocampal neurons in culture. Neurosci Lett. 2002; 321(3): 141–144. PMID: 11880192

69. Yang SH, Sharrocks AD. Convergence of the SUMO and MAPK pathways on the ETS-domain transcription factor Elk-1. Biochem Soc Symp. 2006; 73: 121–129.

70. Demir O, Kurnaz IA. Wildtype Elk-1, but not a SUMOylation mutant, represses egr-1 expression in SH-SY5Y neuroblastomas. Neurosci Lett. 2008; 437(1): 20–24. PMID: 18434015

71. Leight ER, Murphy JT, Fantz DA, Pepin D, Schneider DL, Ratliff TM et al. Conversion of the LIN-1 ETS protein of *C. elegans* from a SUMOylated transcriptional repressor to a phosphorylated transcriptional activator. Genetics 2015; 199(3): 761–775. doi: 10.1534/genetics.114.172668 PMID: 25567989

72. Qin L, Liao L, Redmond A, Young L, Yuan Y, Chen H et al. The AIB1 Oncogene Promotes Breast Cancer Metastasis by Activation of PEA3-Mediated Matrix Metalloproteinase 2 (MMP2) and MMP9 Expression. Mol. Cell. Biol. 2008, vol28, p5937–5950.

73. Greenall A, Willingham N, Cheung E, Boam DS, Sharrocks AD. DNA binding by the ETS-domain transcription factor PEA3 is regulated by intramolecular and intermolecular protein protein interactions. J Biol Chem. 2001; 276(19): 16207–16215. doi: 10.1074/jbc.M011582200 PMID: 11278941

74. Hippenmeyer S, Vrieseling E, Sigrist M, Portmann T, Laengle C, Ladle DR et al. A developmental switch in the response of DRG neurons to ETS transcription factor signaling. PLoS Biol. 2005; 3(5): e159. doi: 10.1371/journal.pbio.0030159 PMID: 15836427

75. Maroulakou IG, Bowel DB. Expression and function of Ets transcription factors in mammalian development: a regulatory network. Oncogene 2000; 19: 6432–6442. doi: 10.1038/sj.onc.1204039 PMID: 11175359

76. Paratore C, Brugnoli G, Lee HY, Suter U, Sommer L. The role of the ETs domain transcription factor Erm in modulating differentiation of neural crest stem cells. Dev Biol. 2002; 250(1): 168–180. PMID: 12297104

77. Lin JH, Saito T, Anderson DJ, Lance-Jones C, Jessell TM et al. Functionally related motor neuron pool and muscle sensory afferent subtypes defined by coordinate ETS gene expression. Cell 1998; 95(3): 393–407. PMID: 9814709

78. Haase G, Dessaud E, Garces A, de Bovis B, Birling M, Filippi P et al. GDNF acts through hPea3 to regulate cell body positioning and muscle innervation of specific motor neuron pools. Neuron 2002; 35 (5): 893–905. PMID: 12372284

79. Helmbacher F, Dessaud E, Arber S, deLapeyriere O, Henderson CE, Klein R et al. Met signaling is required for recruitment of motor neurons to Pea3-positive pools. Neuron 2003; 39(5): 767–777. PMID: 12948444

80. Znosko WA, Yu S, Thomas K, Molina GA, Li C, Tsang W et al. Overlapping functions of Pea3 ETS transcription factors in FGF signaling during zebrafish development. Dev. Biol. 2010; 342(1): 11–25. doi: 10.1016/j.ydbio.2010.03.011 PMID: 20346941

81. Weisinger K, Kavam G, Missulawin-Drillman T, Sela-Donenfeld D. Analysis of expression and function of FGF-MAPK signaling components in the hindbrain reveals a central role for FGF3 in the regulation of Krox20, mediated by Pea3. Dev Biol. 2010; 344(2): 881–895. doi: 10.1016/j.ydbio.2010.06.001 PMID: 20553903

82. Lai KO and Ip NY. Synapse development and plasticity: roles of ephrin/Eph receptor signaling. Curr Opin Neurobiol. 2009; 19(3): 275–283. doi: 10.1016/j.conb.2009.04.009 PMID: 19497733

83. Arber S, Ladle DR, Lin JH, Frank E, Jessell TM. ETS gene ER81 controls the formation of functional connections between group Ia sensory afferents and motor neurons. Cell 2000; 101(5): 485–498. PMID: 10850491

84. Ottone C, Krusche B, Whitby A, Clements M, Quadrato G, Pitulescu ME et al. Direct cell-cell contact with the vascular niche maintains quiescent neural stem cells. Nat Cell Biol. 2014; 16(11): 1045–1056. doi: 10.1038/ncb3045 PMID: 25283993

85. Kawamura K, Kawamura N, Fukuda J, Kumagai J, Hsueh AJ, Tanaka T. Regulation of preimplantation embryo development by brain-derived neurotrophic factor. Dev Biol. 2007; 311(1): 147–158. doi: 10.1016/j.ydbio.2007.08.026 PMID: 17880937

86. Pueschel AW, Adams RH, Betz H. Murine semaphoring D/collapsin is a member of a diverse gene family and creates domains inhibitory for axonal extension. Neuron 1995; 14: 941–948. PMID: 7748561

87. Endo R, Saito T, Asada A, Kawahara H, Ohshima T, Hisanaga S. Commitment of 1-methyl-4-phenylpyrinidinium ion-induced neuronal cell death by proteasome-mediated degradation of p35 cyclin-dependent kinase 5 activator. J Biol Chem. 2009; 284: 26029–26039. doi: 10.1074/jbc.M109.026443 PMID: 19638632

88. Derfuss T, Parikh K, Velhin S, Braun M, Mathey E, Krumbholz M et al. Contactin-2/TAG-1-directed autoimmunity is identified in multiple sclerosis patients and mediates gray matter pathology in animals. Proc Natl Acad Sci 2009; 19: 8302–8307.

89. Gu C, Shim S, Shin J, Kim J, Park J, Han K et al. The EphA8 receptor induces sustained MAP kinase activation to promote neurite outgrowth in neuronal cells. Oncogene 2005; 24: 4243–4256. doi: 10.1038/sj.onc.1208584 PMID: 15782114

90. Prestoz L, Chatzopoulou E, Lemkine G, Spassky N, Lebras B, Kagawa T et al. Control of axonophilic migration of oligodendrocyte precursor cells by Eph-ephrin interaction. Neuron Glia Biol 2004; 1: 73–83. doi: doi:10.1017/S1740925X04000109 PMID: 18634608

91. Quan W, Kim JH, Albert PR, Choi H, Kim KM. Roles of G protein and beta-arrestin in dopamine D2 receptor-mediated ERK activation. Biochem Biophys Res Commun 2008; 377: 705–709. PMID: 18940181

92. Rugarli EI, Ghezzi C, Valsecchi V, Ballabio A. The Kallmann syndrome gene product expressed in COS cells is cleaved on the cell surface to yield a diffusible component. Hum Mol Genet 1995; 5: 1109–1115.

93. Hauser S, Bickel L, Weinspach D, Gerg M, Schaefer MK, Pfeifer M et al. Full-length L1CAM and not its Δ2Δ27 splice variant promotes metastasis through induction of gelatinase expression. PLoS One 2011; 6: 18989.

94. Takino T, Nakada M, Miyamori H, Watanabe Y, Sato T, Gantulga D et al. JSAP1/JIP3 cooperates with focal adhesion kinase to regulate c-Jun N-terminal kinase and cell migration. J Biol Chem. 2005; 280: 37772–37781. doi: 10.1074/jbc.M505241200 PMID: 16141199

95. Kim KY, Kovács M, Kawamoto S, Sellers JR, Adelstein RS. Disease-associated mutations and alternative splicing alter the enzymatic and motile activity of nonmusclemyosins II-B and II-C. J Biol Chem 2005; 280: 22769–22775. doi: 10.1074/jbc.M503488200 PMID: 15845534

96. Korja M, Jokilammi A, Salmi TT, Kalimo H, Pelliniemi TT, Isola J et al. Absence of polysialylated NCAM is an unfavorable prognostic phenotype for advanced stage neuroblastoma. BMC Cancer 2009; 9: 57. doi: 10.1186/1471-2407-9-57 PMID: 19222860

97. Perrin FE, Boniface G, Serguera C, Lonjon N, Serre A, Prieto M et al. Grafted human embryonic progenitors expressing neurogenin-2 stimulate axonal sprouting and improve motor recovery after severe spinal cord injury. PLoS One 2010; 5: 1–7.

98. Diolaiti D, Bernardoni R, Trazzi S, Papa A, Porro A, Bono F et al. Functional cooperation between TrkA and p75(NTR) accelerates neuronal differentiation by increased transcription of GAP-43 and p21 (CIP/WAF) genes via ERK1/2 and AP-1 activities. Exp Cell Res 2007; 313: 2980–2992. doi: 10.1016/j.yexcr.2007.06.002 PMID: 17619016

99. Custer AW, Kazarinova-Noyes K, Sakurai T, Xu X, Simon W, Grumet M et al. The role of the ankyrin-binding protein NrCAM in node of Ranvier formation. J Neurosci 2003; 23: 10032–10039. PMID: 14602817

100. He Z, Tessier-Lavigne M. Neuropilin is a receptor for the axonal chemorepellentSemaphorin III. Cell 1997; 90: 739–751. PMID: 9288753

101. Jones KR, Reichardt LF. Molecular cloning of a human gene that is a member of the nerve growth factor family. Proc Natl Acad Sci 1990; 87: 2060–2064.

102. Ryu H, Lee JH, Kim KS, Jeong SM, Kim PH, Chung HT. Regulation of neutrophil adhesion by pituitary growth hormone accompanies tyrosine phosphorylation of Jak2, p125FAK, and paxillin. J Immunol 2000; 165: 2116–2123. PMID: 10925297

103. Yukawa K, Tanaka T, Bai T, Ueyama T, Owada-Makabe K, Tsubota Y et al. Semaphorin 4A induces growth cone collapse of hippocampal neurons in a Rho/Rho-kinase-dependent manner. Int J Mol Med 2005; 16(1): 115–118. PMID: 15942687

104. Huang P, Kishida S, Cao D, Murakami-Tonami Y, Mu P, Nakaguro M et al. The neuronal differentiation factor NeuroD1 downregulates the neuronal repellent factor Slit2 expression and promotes cell motility and tumor formation of neuroblastoma. Cancer Res 2011; 71: 2938–2948. doi: 10.1158/0008-5472.CAN-10-3524 PMID: 21349947